1 **GRAPHENE-FAMILY NANOMATERIALS IN WASTEWATER TREATMENT**

2 **PLANTS**

3   Octavio Suárez-Iglesias[a], Sergio Collado[a], Paula Oulego[a], Mario Díaz[a,*]

4   [a]Department of Chemical and Environmental Engineering, University of Oviedo,

5   c/Julián Clavería s/n, E-33071, Oviedo, Spain

6   *Corresponding author's e-mail: mariodiaz@uniovi.es

7   *Phone: +34 985 10 34 39; Fax: +34 985 10 34 34

8

9

10

11

12

13

14

15

16

17

18

1

1 **Abstract**

2 The release of graphene and its derivatives in soil, air and water seems an inevitable

3 consequence of the massive future use of these carbonaceous allotropes. From an

4 environmental engineering point of view, it should be noted that part of the aqueous

5 streams containing these nanomaterials will end up in wastewater treatment plants, and

6 there will be interactions between the nanomaterials, the other pollutants in the sewage

7 and the microorganisms of the secondary treatment, which could affect the effectiveness

8 of the depuration process. The present work reviews the available literature on the

9 behaviour of these nanoallotropes in wastewater treatment plants (a literature which is

10 almost exclusively focused on graphene oxide and reduced graphene oxide), and also

11 includes research dealing with simpler systems: i) graphene in purified water, ii)

12 graphene in purified water with salt, and iii) graphene in purified water with organic

13 matter and salt. It is probable that the fate of most of the graphene-family nanomaterials

14 will be the primary/secondary sludge, and that a small portion (mainly in the form of

15 graphene oxide) will pass to the tertiary treatment. Besides, graphene oxide has a

16 negative effect on the biological treatment.

17 **Keywords:** Graphene, nanomaterials, natural waters, sewage, wastewater treatment

18 plants

19 **<u>Nomenclature</u>**

20 Anaerobic ammonium oxidation: anammox,

21 Chloridion intercalated nanocrystallined Mg/Al layered double hydroxides: LDH-Cl,

22 Colloidal quantum dots: CQDs,

1   Dissolved ammonia: NH_4^+,

2   Dissolved oxygen: DO,

3   Dissolved phosphorus: P,

4   Few-layer graphene: FLG (2 – 5 layers),

5   Few-walled nanotubes: FWNT,

6   Five-day biological oxygen demand: BOD_5,

7   Graphene oxide: GO,

8   Graphene quantum dots: GQDs,

9   Graphene-family nanomaterials: GFNs,

10   Multilayer graphene: MLG (2 – 10 layers),

11   Multiwall nanotubes: MWNT.

12   Nanocrystalline Mg/Al layered double hydroxides: $LDH-CO_3$,

13   Natural organic matter: NOM,

14   Phosphates: PO_4^{3-},

15   Pristine graphene: pGr,

16   Reactive oxygen species: ROS,

17   Reduced graphene oxide: RGO,

1   Single-walled nanotubes: SWNT,

2   Total organic carbon: TOC,

3   Total suspended solids: TSS,

4   Ultraviolet: UV,

5   Volatile suspended solids: VSS,

6   Wastewater treatment plants: WWTPs.

7   1. **Introduction**

8   Pristine graphene (pGr) is a two-dimensional structure, formed by hexagonal rings of sp^2-

9   hybridised carbon atoms, which is considered the precursor of the graphene-family

10   nanomaterials (GFNs) and other families of carbon nanoallotropes [1,2]. Regarding to the

11   first group, GFNs, a monolayer graphene sheet can be oxidised to form graphene oxide

12   (GO) or packed in parallel with other sheets to form few-layer graphene (FLG, $2-5$

13   layers), multilayer graphene (MLG, $2-10$ layers) and graphite nanoflakes (uncountable

14   number of layers, but with a thickness and/or lateral dimension less than 100 nm). The

15   packing of an "infinite number" of layers generates graphite, which is a carbon

16   nanoallotrope but is not a member of the GFNs. Regarding this second group (materials

17   which do not belong to the GFNs), one graphene sheet can be cut following certain

18   pattern and folded to build regular polyhedrons, called fullerenes; or rolled up to form

19   single-walled nanotubes (SWNT). Additionally, FLG and MLG can be cut and wrapped

20   up to build few-walled and multiwalled fullerenes (called onion-like carbon

21   nanoparticles), or rolled up to form few-walled and multiwalled nanotubes (FWNT and

22   MWNT, respectively). Fig. 1 represents some of these allotropes.

2   Due to its exceptional electrical and physical properties, pGr is suitable for applications

3   in high-speed electronics, data storage devices, flexible touch screens, supercapacitors,

4   solar cells and electrochemical sensors [3,4]. Research on GFNs had been done since the

5   XIX century, but the interest for them started to grow in 2004 – 2005, when Novoselov

6   and coworkers isolated pGr and reported its unique behaviour [5,6]. pGr can be obtained

7   from graphite by dry mechanical exfoliation with an adhesive tape, by exfoliation in

8   solvents with ultrasounds or by chemical intercalation of alkali metals between the sheets

9   [7]. Graphene is also produced by deposition of the vapour generated after the thermal

10 decomposition of carbon-containing substances on a metal surface (that catalyses the

11 rearrangement of the vapour to form sp^2 carbon species), by heating of silicon carbide

12 and by sonication in water of graphite oxide followed by reduction [7,8], being this last

13 one the most popular. Graphite oxide is usually generated from graphite by the so-called

14 Hummers' process (oxidation using potassium permanganate, sodium nitrate, and sulfuric

15 acid), and is a material which displays a structure similar to that of graphite, but contains

16 hydroxyl and epoxy groups in the basal planes and carboxyl groups in the edges of the

17 sheets. The single layers obtained after this exfoliation are not of pGr, but of GO, and it

18 has to be subjected to chemical reduction to eliminate the oxygen-bearing functionalities

19 [6,9,10]. Nonetheless, the product of this reduction commonly presents several defects in

20 the honeycomb lattice, besides some functional groups resist the reduction, and therefore,

21 it is named reduced graphene oxide (RGO) instead of pGr [9,11]. GFNs, especially GO

22 and RGO, have proved to be effective for water remediation and adsorption of noxious

23 gases [12-14]. A schematised picture of RGO is also shown in Fig. 1.

24 The increasing production of GFNs raised concerns about their potential health and

25 ecological risks in the early 2010s [15,16]. Furthermore, the higher the commercialised

1 amounts of graphene, the higher the amount of GFN-containing wastes that will be

2 released into sewages, and therefore, greater concentrations of these materials can be

3 expected in the influent to wastewater treatment plants (WWTPs), since these facilities

4 are the final destination of most of the residual liquid effluents from industrial and urban

5 areas. Unfortunately, quantifications of the aforesaid concentrations are not available yet,

6 unlike those of metallic nanoparticles, nanotubes or fullerenes [17]. A flow diagram of

7 the different stages of a WWTP is shown in Fig. 2.

8   FIGURE 2

9 Initially, screens composed of gratings, wire meshes, perforated plates or parallel bars,

10 rods or wires separate the coarser solids, whereas grit chambers remove sand, gravel,

11 cinders and particles with sedimentation velocities considerably higher than those settling

12 in the primary clarifier [18]. In order to facilitate the aggregation/flocculation of the

13 remaining suspended solids, a coagulant can be added (such as iron or aluminium or salts,

14 or long-chain polyelectrolytes). After the separation of the primary sludge, which is

15 mostly formed by highly putrescible matter, a biological step removes the dissolved

16 organic compounds that are easily biodegradable. This biological process, also called

17 secondary treatment, is usually carried out by means of activated sludge, a suspension of

18 aerobic microorganisms that use these substances as feed for metabolic processes and for

19 number growing. If elimination of dissolved ammonia and phosphorus is required, the

20 activated sludge reactor is combined with an anoxic one (or with a succession of anoxic

21 and aerobic devices) to facilitate nitrification/denitrification and enhanced phosphorus

22 removal [19,20]. Since the growth of the mass/volume of the microorganisms during this

23 stage is undesirable, part of them are purged from the secondary sedimentation tank. The

24 clarified water can be subjected to tertiary treatment (depth filtration, membranes,

25 adsorption, gas stripping, ion exchange and advanced oxidation) as well as to a final

1   disinfection by means of ozone, ultraviolet light or chlorine/chlorinated chemicals [18].

2   Sludges from the primary and secondary clarifiers are frequently mixed and digested

3   anaerobically, in order to obtain a stabilised biosolid and biogas (mainly comprised of

4   methane and carbon dioxide), which can be employed to generate electricity and heat

5   [21]. Digested biosolids are dewatered and sent to landfill, together with coarser solids

6   and grit. Water streams and sludge are characterised in terms of pH, electrical

7   conductivity, turbidity, total suspended solids (TSS), volatile suspended solids (VSS),

8   total organic carbon (TOC), 5-day biological oxygen demand (BOD_5), dissolved oxygen

9   (DO), dissolved ammonia (NH_4^+), dissolved phosphorus (P) or phosphates (PO_4^{3-}) and

10 the number of bacteria.

11 The aim of this review is to compile all the literature dealing with the performance of

12 GFNs in the different steps of a WWTP. Due to the shortage of publications on the topic

13 of wastewater system, some works focused on natural water and simple aqueous mixtures

14 have been included, as they provide information which could be extrapolated to

15 wastewater. As will be seen, GO and RGO have been the most studied compounds of the

16 family, whereas very few papers have been written on pGr and FLG.

17   2.   **Piping and pretreatment**

18 There is a scarcity of literature that can be related to the matter of this section, and almost

19 all is devoted to GO, because it is more hydrophilic than pGr or RGO, due to its O-

20 containing groups. Among these papers, those of Chowdhury and co-workers on

21 deposition and release onto silica and silica coated with poly-*L*-lysine [22], aluminium

22 oxide and silica coated with natural organic matter (NOM) [23] surfaces can be cited.

23 Although their objective was to acquire some knowledge about the behaviour of GO in

24 sediments and soils, the tests were not implemented in soil matrices (whose properties are

25 very different from wastewater), but in simple mixtures of deionized water + one

1   electrolyte + GO, using a quartz crystal microbalance with dissipation monitoring, which

2   allows a more general interpretation of the interactions between surfaces and nanosheets.

3   In this regard, deposition importance followed the decreasing order NOM-coated silica>

4   metal ≈ poly-*L*-lysine-coated silica > silica, because both silica and GO were negatively

5   charged at the working pH, both Al_2O_3 and poly-*L*-lysine were positively charged and

6   NOM is able to adsorb GO in spite of being negatively charged too (as will be further

7   explained in the next section). Ionic strength and salt type (NaCl, $CaCl_2$, $MgCl_2$)

8   influence the process. After introducing deionised water to decrease the ionic strength

9   (simulating rainfall and flooding events which are very common in natural

10 environments), all surfaces display significant release of deposited GO, indicating that the

11 deposition was highly reversible. The effect of aqueous GO concentration was only

12 estimated on silica coated with poly-*L*-lysine [22], where the increase from 1 mg/L to 10

13 mg/L GO caused an increase in the deposited mass at 10 mmol/L NaCl (measured as

14 frequency shifts of the balance and not as milligrams) and a decrease in the fraction

15 released (from 45% to 25%) after the introduction of deionized water.

16 However, these works only suggest that part of the GO could be united to metallic coarse

17 solids and to sand (which are expected to be coated by organics when submerged in

18 wastewater), and could be removed in the screens and in the grit chamber, respectively.

19 No information on how the water flow and the aqueous organic content affect amount of

20 deposited/released graphene was provided (factors that cannot be very important in

21 sediments and soils subjected to natural water, but are critical in wastewater treatment).

22 Fortunately, Hua et al. [24] carried out some research in this field that can be useful, since

23 they also utilized simple model systems instead of complex matrices. They mixed

24 solutions containing distilled water + GO, distilled water + NOM + GO, distilled water +

25 electrolyte + GO and distilled water + NOM + electrolyte + GO with a sand bed, stirred

1 the mixture, allowed it to stand for 2 h. These authors also introduced similar solutions

2 but without GO and let the system stand for 24 h. GO concentrations were determined by

3 spectrophotometry. Several shear flows were simulated (but soft enough to avoid

4 resuspension of the sand), obtaining a rapid release of the graphene in the systems which

5 did not contain electrolyte. In the systems with $CaCl_2$ + NOM or $MgCl_2$ + NOM, the

6 release became more difficult (especially with Ca^{2+}), and when only the electrolyte was

7 present, the release of the nanomaterial was even more limited (especially with Ca^{2+}). If

8 the shear rate is so strong that it suspends the sand bed, the GO release was improved.

9 Since the solids in wastewater pipes are in the form of suspensions, with higher

10 concentrations of organic matter and lower concentrations of divalent cations (80 − 260

11 mg/L TOC and 0.15 − 0.40 mmol/L Ca^{2+} or Mg^{2+} [18]) than those reported in the paper

12 of Hua and coworkers (4 − 5 mg/L TOC and 1.5 mmol/L Ca^{2+} or Mg^{2+} [24 - 26]), it

13 seems likely that most of the GO will be detached from the solids, thus passing to the

14 primary treatment. Deposition in the grit chamber due to aggregation/sedimentation (and

15 not to deposition on the sand surface) is unlikely because these systems are designed to

16 remove particles higher than 0.21 − 0.15 mm during residence times of 30 s − 3 min [18],

17 whereas graphene aggregates are several orders of magnitude lower and can remain

18 suspended in water for days, as will be seen in section 3.

19 Other minerals than sand can constitute the grit of the influent, such as kaolin/kaolinite,

20 hematite, montmorillonite, goethite and layered double hydroxides. Adsorption studies of

21 GO in deionised water (and in absence of electrolytes and NOM), revealed that GO can

22 interact with double layered hydroxides [27], hematite [28] and goethite, but not with

23 montmorillonite [29]. Interactions with kaolin or kaolinite are possible [28] or not [29],

24 depending on pH and the sizes and concentrations of the GO/mineral particles [29].

25 Taking into account that there is no adsorption of GO on SiO_2 when electrolytes are

1 absent [29], that NOM coatings improve the deposition on silica surfaces [23] but its

2 presence in soluble form hinders the interactions with the suspended minerals [28,31] and

3 that it is not known the effect of water flow in the release of the adsorbed GO, we are

4 incapable of predicting the fate of this adsorbed GO during the pretreatment.

5 On the other hand, Hou et al. [32] proved that GO could be easily reduced to RGO upon

6 exposure to sunlight, although the resulting species were more fragmented than the

7 starting nanomaterial and showed lower molecular weights. This fact, along with the

8 ability of some bacteria [33] and naturally occurring organics [34], sulfides [35] and

9 ferrous iron [36] to reduce GO as well, indicates that the majority of GO released to the

10 environment could became RGO after certain time. In this regard, Chowdhury et al. [37]

11 used the quartz crystal microbalance with dissipation monitoring to analyse the

12 deposition and release onto silica and NOM-coated silica surfaces of GO aerobically

13 photoreduced for 1, 3, 11, 61 and 187 hours, and anaerobically photoreduced for 3, 11

14 and 61 hours. In all the cases, phototransformed species showed considerably lower

15 deposition than control GO, being negligible their deposition on silica. The longer the

16 irradiation time, the lower the deposition on NOM-coated surfaces, regardless of the

17 presence or absence of air. Nevertheless, when deionised water was introduced to

18 decrease the ionic strength, phototransformed species gave lower amounts of released

19 material than control GO, indicating that the few amounts of deposited nanomaterial were

20 more strongly attached to the NOM-coated silica. The longer the irradiation time, the

21 lower the amount released. Anaerobically photoreduced GO was more irreversibly

22 deposited than the aerobically one. So, by extrapolation, it can be inferred that, if there

23 were low amounts of GO bound to the coarse solids and to the sand, there will be less

24 RGO. However, due to the hydrophobicity of the reduced species, they could

25 agglomerate through van der Waals forces more readily than GO, and a fraction of them

1 could settle in the grit chamber, since, in some cases, sedimentation in deionised water

2 after reduction took place in minutes [36]. Notwithstanding the foregoing, according to

3 Chowdhury et al. [37], NOM improves the stability of deionised water + electrolyte +

4 RGO, and keeping in mind the relatively high amount of organic matter contained in the

5 sewage, the reduced nanomaterial settled down together with the grit will be little if

6 adsorption on other minerals than sand is not very strong (to the best of our knowledge,

7 there are not studies similar to those of GO with kaolin/kaolinite, hematite,

8 montmorillonite, goethite and layered double hydroxides for RGO).

9 Surfactants, which are commonly found in wastewater, also stabilize aqueous

10 suspensions of pGr, RGO and GO [38, 39]. They are adsorbed on the nanomaterial

11 surface, increasing both electrostatic repulsion (because expansion of the electrical

12 double layer) and steric hindrance (because the size of the surfactant molecule) between

13 sheets.

14   3. **Primary treatment**

15 In opposition to pretreatment, where no literature dealing with wastewater exists, three

16 papers have been found that contain data on the sedimentation behaviour of GFNs

17 suspended in sewage: those by Chowdhury et al. [40], and Ren et al. [31] for GO and that

18 by Chowdhury et al. [41] for RGO.

19 Chowdhury et al. [40] prepared a synthetic urban wastewater containing 100 mg/L of

20 TOC by dissolving 160 mg of peptone, 110 mg of meat extract, 30 mg of urea, 28 mg of

21 K_2HPO_4, 7 mg of NaCl, 4 mg of $CaCl_2·2H_2O$ and 2 mg of $Mg_2SO_4·7H_2O$ in a litre of

22 deionised water. They added around 10 mg/L of GO to it and studied the evolution with

23 time of both the GO concentration and the size of its aggregates (through the

1   measurement of the hydrodynamic diameter) in a 20 mL borosilicate glass bottle.

2   Furthermore, they compare these results with those obtained by introducing GO into a

3   synthetic solution without meat extract or urea, with those of the hypothetical effluent

4   from a WWTP (prepared by diluting the synthetic wastewater to achieve 15 mg/L of

5   TOC) and with those of the actual effluent from the WWTP of North Oconee, Athens,

6   Georgia (pH 6.8, 5 ppm of TSS, 6.5 mg/L of TOC, 881 μS/cm of conductivity, 0.1 mg/L

7   of NH_4^+). Fig. 3 shows their main findings. In three of the four solutions, more than 90%

8   of GO remained suspended for 28 days, being the most stable that with the synthetic

9   wastewater (although the measured concentrations were higher than that at the beginning

10 because of the interference of the organic matter with the UV-vis spectroscopy employed

11 for measuring the GFNs). The immediate settling of more than 30% of GO and its total

12 sedimentation after one day in the Oconee effluent was attributed to its high conductivity

13 and to the presence of residual coagulant in the treated water. Supplementary experiments

14 in single-salt solutions had indicated that the hydrodynamic diameter of GO augmented

15 with electrolyte concentration (NaCl, $MgCl_2$ or $CaCl_2$) and that, for a fixed electrolyte

16 concentration, it decreased when increasing amounts of organic matter (humic acid) were

17 added, but Fig. 3b proves that these trends cannot be extrapolated to complex mixtures.

18   FIGURE 3

19 The same synthetic urban wastewater than Chowdhury and coworkers [40] was employed

20 by Ren et al. [31]. Moreover, they pointed out that the conductivity and pH values of this

21 synthetic sewage were 74 μS/cm and 6.78 units, respectively. The main aim of these

22 researchers was to assess the influence of Al_2O_3 particles ($0.3 - 0.074$ mm) on a

23 suspension containing initially 6 mg/L of GO after 24 h. This aluminium oxide was

24 selected because it is present in common naturally occurring minerals, as kaolinite and

12

1 gibbsite, and is able to adsorb GO on its surface, leading to a faster sedimentation of the

2 GFN since the alumina particles are orders of magnitude higher than those of GO. So, in

3 the absence of Al_2O_3, no appreciable settling of the dissolved graphene took place, but

4 when 10000 mg/L of Al_2O_3 were added to the wastewater before the 24 h period, the

5 remaining GO concentration was 5.2 mg/L. Nonetheless, these results were almost the

6 same than those obtained in Milli-Q water (3.6 μS/cm, 0 mg/L of TOC, pH 7.12), which

7 proved that the dissolved organic matter prevented the GO aggregation despite the

8 presence of electrolytes. Further experiments in natural water (from Dongpu Lake, Hefei,

9 Anhui, China, 105 μS/cm, 3.7 mg/L of TOC, pH 7.55), synthetic groundwater (220

10 μS/cm, 0 mg/L of TOC, pH 7.9) and synthetic surface water (75 μS/cm, 0 mg/L of TOC,

11 pH 7.92) gave values of GO after 24 h lower than 0.6 mg/L in absence of aluminium

12 oxide and lower than 0.2 mg/L in its presence.

13 With regard to RGO, Chowdhury et al. [41] chemically reduced GO for 1, 2 and 5 h and

14 tested the settling ability of the obtained RGOs in the same synthetic wastewater and

15 WWTP effluent where they carried out experiments with GO. The O:C ratios of GO, 1 h–

16 RGO, 2 h–RGO and 5 h–RGO were 0.42, 0.32, 0.26 and 0.17, respectively. Contrarily to

17 what happened with the photoreduction described in the previous section, chemical

18 reduction did not significantly fragment the graphene flakes. Fig. 4 displays the results of

19 the investigation. In the Oconee effluent, the evolution of the suspended RGO

20 concentration with time is very similar to that of GO in Fig. 3a, and it was attributed to

21 the high conductivity of the water and to the possible presence of coagulant as well.

22 However, in the synthetic wastewater, partially reduced species settled quicker than GO.

23 In this case, hydrodynamic diameters were not determined.

24 FIGURE 4.

13

1   Studies in lab mixtures of deionised water + GFN, deionised water + electrolyte + GFN

2   and deionised water + electrolyte + NOM + GFN offer the following explanations to the

3   Fig. 3 and Fig. 4: hydroxyl and carboxyl groups of the GFN are deprotonated at

4   environmentally relevant pH values, so monovalent cations screen them (favouring the

5   van der Waals attraction between the nanomaterial sheets) and divalent cations form

6   bridges between the groups of different sheets generating stronger attraction than

7   screening [42]. Higher conductivities imply higher amounts of cations, and therefore,

8   higher attraction, higher aggregation and quicker settling. The anion associated to the

9   cation also interacts with the nanoflake, making the GFN more negatively charged, but it

10   seems that, when the electrolyte concentration increases, cations have a more pronounced

11   effect on the suspension behaviour than anions do [31]. Regarding NOM, GFNs readily

12   adsorb it on those areas of the basal plane without oxygenated groups via hydrophobic

13   interactions or π - π bonding [12], and two opposing processes could happen: better

14   aggregation (because organic matter is negatively charged, and provided more binding

15   sites for cations) or steric hindrance (due to the size of the adsorbed organic molecules,

16   which hampers the aggregation of the nanosheets), but the second one is the predominant

17   in simple solutions [24,35,37,40,41]. Furthermore, adsorption of organic matter might

18   cover the oxygen-containing groups of GO, obstructing the reduction process [35]. On

19   the other hand, RGO has less −COOH and −OH groups than GO, which allows for less

20   screening, fewer cation bridges and greater adsorption of NOM, but makes it more

21   hydrophobic. So, the data showed in Fig. 4b are the result of the combination of the two

22   opposing effects: i) GO remains suspended in synthetic wastewater due to its low

23   conductivity (and, to a lesser extent, to the steric repulsion caused by the adsorbed

24   organic matter, as can be inferred from Fig. 3a); ii) RGO settles because of the van der

25   Waals attraction (an attraction that the adsorbed organics are not able of hindering).

14

Nonetheless, in other complex systems, such as simulated surface water (containing 16.5

mg/L of $MgCl_2$, 8.3 mg/L of $MgSO_4$, 3 mg/L of $KHCO_3$, 19.3 mg/L of $NaHCO_3$, 33

mg/L of $CaCO_3$ and 5 mg/L of humic acid) the 5 h–RGO completely settles after 1 day

and control GO after 7 days, but 36% of the 1 h–RGO and 7% of the 2 h–RGO remained

suspended after 27 days, indicating that the humic acid, under certain circumstances,

impeded the van der Waals attractions when the oxide is partially reduced.

Simple lab mixtures have also been utilised to determine the influence of ultraviolet (UV)

radiation, sunlight and low-molecular-weight organic acids on the hydrodynamic size of

GFNs and the effect of sulphides, ferrous iron and several colloidal minerals on the

settling of GO. Andryushina et al. [43] illuminated a suspension of 25 mg/L of GO in

distilled water (pH adjusted to 6) with UV light at wavelengths from 310 to 390 nm and

1.2×10^{17} quanta/s intensity for 180 min and reported on a photoreduction of the GFN

which increased with the illumination time. A non-monotonous evolution of the

hydrodynamic size (320 nm at 0 min, 520 nm at 30 min and 280 nm at 180 min) as result

of the disappearance of the hydrogen bonds, the intercalation of water molecules and the

final apparition of π - π interactions, was observed. Chowdhury et al. [37] used a solar

simulator (290 – 700 nm wavelength, 650 W/m^2 intensity) to photoreduce GO both

aerobically and anaerobically in purified water at pH 5.5 for 500 h, noticing that the

presence or absence of air did not influence the process significantly and that the

hydrodynamic diameter decreased with the irradiation time (due to the breakage of the

nanosheets into smaller fragments) from 190 to 110 nm at 200 h, but remained constant

between 200 and 500 h. Nevertheless, when the particles phototransformed for 1, 3, 11,

68 and 187 h were placed in purified water + electrolyte and in purified water +

electrolyte + humic acid for several minutes, it was seen that the aggregation rate was a

function of the irradiation time, which anaerobically reduced the material aggregated

1 faster than the GFN aerobically treated. Besides, NOM hindered this aggregation. Hu et

2 al. [44] left a suspension of highly reduced RGO (100 mg/L) in pure water for 120 days

3 within a visible-light incubator (intensity of 34 W/m^2 and relative humidity of 80%), and

4 instead of a reduction, they reported on the increase of the O:C ratio from 0.064 to 0.099,

5 the decrease of both the hydrodynamic diameter and the aggregation rate, the apparition

6 of numerous defects and a drop of the toxicity to the microalga *Chlorella vulgaris*. The

7 properties of another similar suspension, but covered with aluminium foil during the 120

8 days, were intermediate between those of the RGO and those of the photo-oxidised

9 species. Wang et al. [45] added 0, 1, 10 and 40 mg/L of gallic or benzoic acid to solutions

10 containing 1 and 5 mg/L of RGO (since low-molecular-weight acids are typically used in

11 several manufactured products and contribute a considerable proportion of NOM), and

12 after a period of 96 h, it was noticed that the hydrodynamic diameters of the aggregates in

13 the water + gallic acid + RGO systems were lower than in the mixtures made up of water

14 + RGO and water + benzoic acid + RGO. Thus, the higher the gallic acid concentration,

15 the lower the aggregate size and the higher the RGO content, the higher the

16 hydrodynamic diameter. It was not indicated if there was significant sedimentation of the

17 graphenous material. Moreover, the suspensions without acid inhibited the growth of the

18 green alga *Scenedesmus obliquus* to a greater extent than those containing 1 and 10 mg/L

19 of acid, but not as much as those with 40 mg/L of acid, and inhibitions were lower for

20 benzoic acid than for gallic acid, pointing out that there was no direct correlation between

21 the aggregation and the algal toxicity. Fu et al. [35] simulated a partial natural reduction

22 of GO in anaerobic aquifers and sediments by a strong reductant (S^{2-}), using an aqueous

23 suspension of 10 mg/L of GO in 50 mmol/L Tris-HCl (pH buffer), and 500 mmol/L Na$_2$S

24 (previously prepurged with nitrogen). The colour of the suspension changed from brown

25 to black within 1 h, started to settle within 2 h and it was fully settled at 12 h. Subsequent

1   redispersion tests in deionised water demonstrated that the longer the reaction time, the

2   lower the O:C ratio and the lower the stability of the suspensions. If NOM was added (20

3   mg/L of TOC), no noticeable sedimentation occurred within the 48 h period that lasted

4   the experiments. When the pH was varied in the NOM-free mixtures, both the stability of

5   the suspensions and the O:C ratios followed the order pH 8.7 >> pH 5.7 > 7.4, indicating

6   a non-monotonous dependence of the Na_2S reduction efficiency with pH. Wang et al.

7   [36] studied the partial reduction of GO in an anoxic medium as well, but in presence of

8   the mild reductant Fe(II). After removing the dissolved oxygen from a GO suspension of

9   125 mg/L and reducing it with 4, 10 or 40 mmol/L of Fe^{2+} for 15 h, new suspensions of

10 50 mg/L of GFN in deionised water or deionised water + 10 mmol/L NaCl were prepared

11 and they were settled for 40 h in the dark, concluding that the stability decreased in the

12 order GO > $RGO_{(4\ mmol/L\ Fe)}$ > $RGO_{(10\ mmol/L\ Fe)} \geq RGO_{(40\ mmol/L\ Fe)}$. The ionic strength had

13 little influence on it and the sedimentation was fast during the first minutes but reached a

14 plateau beyond 2 h (so, the RGOs still possessed considerable colloidal stability).

15 Additionally, the higher the amount of the reducing agent, the lower the O:C ratios, but

16 the higher the adsorption affinity for bisphenol A, revealing that the RGOs generated by

17 mild reductants could accumulate certain toxic contaminants more easily than GO, and

18 transport them farther away than the RGOs produced by strong reductants, which were

19 less stable. Zou et al. [27] tested the ability of naturally occurring fine mineral particles,

20 such as nanocrystallined Mg/Al layered double hydroxides ($LDH-CO_3$) and chloridion

21 intercalated nanocrystallined Mg/Al layered double hydroxides (LDH-Cl) for coagulating

22 a suspension of 60 mg/L of GO in Milli-Q water plus NaCl. pH was varied from 3 to 10,

23 NaCl from 1 to 100 mmol/L, particle concentrations between 250 and 2000 mg/L, contact

24 time between 5 and 240 min and temperature between 20 and 50ºC, observing that the

25 removal efficiency went through a maximum with pH, slightly increased with ionic

1   strength, improved initially with both coagulant concentration and time but levelled off

2   beyond a certain value and went through a minimum with temperature. In all the cases,

3   LDH-Cl was better than LDH-CO_3, perhaps because the first one was more positively

4   charged than the later. Huang et al. [30] performed similar experiments with kaolinite and

5   goethite associated with kaolinite (10% or 4% goethite) in a mixture of deionised water

6   bearing 20 mg/L of GO, 2000 mg/L of mineral and with pH adjustment. It was found

7   that, after 24 h, GO sheets could be aggregated in presence of kaolinite, kaolinite with 4%

8   goethite and kaolinite with 10% goethite if pH was lower than 4, 5 and 6, respectively.

9   The addition of an electrolyte improved the sedimentation process, the removal being

10 around 100% for 50 mmol/L of NaCl.

11 Nanocomposites of GFNs and metal/metal oxides are very common [46 - 48], but there is

12 only one article on the aggregation/sedimentation of TiO_2-RGO in deionised water + pH

13 modifier. Hua et al. [49] observed that, after 240 min settling, the concentration of

14 nanocomposites in the supernatant decreased with increasing pH from 2 to 10, but if

15 $CaCl_2$ was added to the mixture, the drop was more pronounced (specially, beyond pH 5).

16 Hydrodynamic diameters varied between 1500 and 3000 nm in absence of electrolyte, but

17 from 1500 to 13000 nm when it was present. The authors also investigated the effect of

18 irradiating the sample with a UV lamp of 15 W for 40 h, and reported that the higher the

19 irradiation time, the lower the concentration in the supernatant, but after 30 h, the

20 sedimentation rate got worse. Supposedly, UV radiation causes further reduction of the

21 RGO, but beyond 30 h, it separates the nanocomposite into RGO and TiO_2, or

22 photofragments RGO into products of lower size.

23 Finally, it has to be said that Liu et al. [50] and Yang et al. [28] analysed the interactions

24 between GO and several minerals/pollutants, but not with the aim of removing the

1 nanomaterial, but knowing if it was useful as a coagulant for removing the substances

2 present in the water (cationic dyes, hematite, kaolin, humic acid and kaolin + humic

3 acid). However, since these researchers did not determine the concentration of the GO

4 that remains after the flocculation, their works have not been commented in the present

5 review.

6   **4. Secondary treatment**

7 According to section 3, the presence of a coagulant and the natural reduction of GO

8 would lead to a high deposition or content of the GFNs in the primary sludge.

9 Nevertheless, the complex interactions that take place in the wastewater could maintain

10 part of these nanomaterials in suspensions for more than $1.5 - 2.5$ h, which is the

11 common residence time in the primary clarifiers [18]. See, for instance, some of the

12 species in Fig. 4. Then, the graphenous materials would pass to the biological treatment

13 of the WWTP, the microorganisms being exposed to them.

14 The biocidal ability of GFNs has been recently reviewed by Hegab et al. [51]. In short, it

15 is a function of nanosheet size, surface area and roughness, dispersability, hydrophilicity

16 and functional groups present in the nanomaterial, being three the main mechanisms

17 through which this antibacterial activity occurs: i) membrane disruption by the sharp

18 edges of the sheets and phospholipid extraction, ii) generation of reactive oxygen species

19 (ROS) that destroy proteins, DNA and other cellular components and iii) enclosing the

20 bacterium among the nanosheets, isolating it from the medium and preventing it from

21 consuming nutrients. Notwithstanding this, there are a few reports where GO improved

22 the growth of some microorganisms [52].

1   Only three papers have been found dealing with the effect of these nanomaterials on

2   activated sludge. The most relevant information is included in Table 1. Two of them

3   [53,54] are focused on the acute toxicity (high concentrations during short times) of GO

4   to bacteria and the other one [55] on the removal of GO and FLG in the secondary

5   clarifier. Ahmed and Rodrigues [53] reported that the presence of GO deteriorated the

6   purification process (the final effluent had more BOD_5, ammonia nitrogen, phosphate and

7   turbidity) and the sludge quality (which required higher suction times, and therefore, less

8   dewaterability). They did not see bacteria isolation among the nanosheets, but noticed a

9   rise in the production of ROS at concentrations of 200 – 300 mg/L of GO, and suggested

10   that it could be one of the causes of the toxicity. In this sense, Combarros et al. [54]

11   separated cells into "active cells" and "dead cells", and "active cells" into "viable cells"

12   (those with intact membranes) and "damaged cells" (those with damaged membranes, but

13   metabolically active), finding that GO did not induce a significant increase of the dead

14   cells (as expected from ROS generation), but a rise of the damaged cells, probably

15   because of the edges of the GO sheets. They did not see bacteria enclosing either.

16   Yang et al. [55] related the amount of GFN trapped into the biomass (q, mg GFN/g TSS)

17   with the GFN concentration in the clarified effluent (C_L, mg/L) through the Freundlich

18   model and pointed out that, at typical sludge concentrations in WWTP (1000 – 4000

19   mg/L of TSS), the secondary sedimentation depended on the nanomaterial and its

20   concentration, but for 25 mg/L of GFN and a settling time of 30 min, computed removals

21   are in the range of 62 – 94% for GO and of 73 – 91% for FLG. If calculations are done

22   with the model for a GFN concentration as high as 1000 mg/L, removals fall to 14.6 –

23   46.3% in the case of GO, but improve to 79 – 93% in the case of FLG.

24   TABLE 1

1   On the other hand, several publications on GFNs and autotrophic removal of inorganic

2   nitrogen have been found: four articles about anaerobic ammonium oxidation

3   (anammox), where NH_4^+ is transformed into gaseous N_2 using NO_2^- as electron acceptor

4   [56,57], and one article about bioelectrochemical denitrification, where NO_3^- becomes N_2

5   using the H_2 produced by water electrolysis as electron donor [58]. They are all

6   summarised in Table 2. Most of the WWTPs employ the heterotrophic

7   nitrification/denitrification system, where ammonium is oxidised to nitrate in a first

8   aerobic stage, and nitrate reduced to gaseous dinitrogen in a second anaerobic stage.

9   Nonetheless, heterotrophic denitrifiers require organic carbon as food source and generate

10   a high volume of sludge, whereas autotrophs just need inorganic carbon substrates

11   (carbon dioxide or bicarbonate) and their volume does not grow so much. In the case of

12   anammox bacteria, this low growth is a shortcoming for the system start-up. Furthermore,

13   the anammox process is not applicable to wastewater with high C:N ratios, which makes

14   it unsuitable for treating the effluent of the primary clarifier, and only can treat the liquid

15   that results from the dewatering of the anaerobically digested sludge [59], but a

16   combination of activated sludge and anammox has been proposed in order to implement

17   this technique in the main streams [60].

18   TABLE 2

19   In a synthetic wastewater with anammox bacteria and various GO concentrations, Wang

20   et al. [61] saw a maximum removal of NH_4^+ at 100 mg/L of GO and attributed it to the

21   amount of extracellular polymeric substances (EPS), which also went through a

22   maximum at such concentration of GO. EPS are sticky metabolic products excreted by

23   the cells, which can provide nutrition to microorganisms, protect them from toxic shocks

24   and enhance their aggregation and the formation of high-size macroflocs. Wang et al.

[62] also proved that the anammox sludge stored with 100 mg/L of GO at low temperatures removed more nitrogen, settled in a better way, lost less EPS, grew faster and had larger particle size than that stored at room temperature. Yin et al. [63] carried out experiments similar to those of Wang et al. [61] and noticed a change in the colour of the synthetic wastewater, which could be due to the reduction of GO by the anammox microorganisms (note that bacterial reduction has been mentioned in section 2). In order to verify the hypothesis, they added different concentrations of RGO to key enzymes of anammox bacteria (hydrazine dehydrogenase, nitrate reductase and nitrite reductase) and reported that the higher the nanomaterial concentration, the higher the activity of the three enzymes. Moreover, when compared RGO with coenzyme Q (an exogenous coenzyme, whose electron transfer capacity restores the activity of hydrazine dehydrogenase), RGO showed a much better superior performance. Yin et al. [64] attributed the high growth rate of the anammox cells in presence of 100 mg/L of RGO to this effect of the reduced nanomaterial on hydrazine dehydrogenase, which led to a fast start-up of anammox reactors. In contrast to anaerobic ammonium oxidation, Chen et al. [65] informed that hydrogenotrophic denitrification did not suffer any improvement in presence of GO, but a deterioration at 100 and 150 mg/L. Increasing GO concentration caused a reduction in the microbial community richness, a variation of the dominant phyla and classes, a rise in the ROS production and higher membrane damages (evaluated through release of lactate dehydrogenase).

GFNs are also capable of adsorbing heavy metals and toxic organics [66 – 69], facilitating their transport to the biological treatment, although the sheet – sheet aggregation of the nanomaterials also could sequester these substances within the aggregates and reduce their bioavailability [70]. However, this matter has not been addressed by any of the aforementioned authors.

5. Tertiary treatment

As mentioned in the introduction, the effluent from the secondary clarifier can be subjected to further purification by techniques such as depth filtration through a granular medium (mainly sand, anthracite or garnet), membrane filtration (microfiltration, ultrafiltration, nanofiltration and reverse osmosis), adsorption (usually, on activated carbon beds), gas stripping (for removing NH_3, CO_2, H_2S and volatile organic compounds), ion exchange (synthetic resins that exchange NH_4^+, NO_3^-, Cr^{3+}, Ni^{2+}, Cu^{2+}, Zn^{2+}, Cd^{2+} and Pb^{2+} by less harmful ions) and advanced oxidation (through ozone, hydrogen peroxide, supercritical water or Fenton processes). GFNs are widely proposed for manufacturing adsorbents, membranes and ion exchange resins which remove pollutants from wastewater [13,14,73,74], but unfortunately, there is not literature related to the removal of GFNs from aqueous streams by depth filtration, adsorption, membrane filtration or ion exchange. Moreover, since graphenous materials are not dissolved gases, they cannot be removed in the stripping process.

Advanced oxidation of GFNs has received more attention, but all the studies have been carried out in distilled/ultrapure water, without substances that can react with the oxidant and decreased the efficiency of the treatment. Xing et al. [75] oxidised FLG (obtained by deposition of vapour on nickel wafer) with 10 - 0.001 mmol/L of H_2O_2 for $0 - 25$ h at room temperature. Transmission electron microscopy, atomic force microscopy and confocal Raman spectroscopy showed an initial appearance of defects by random attack of the oxidant, followed by progressive attraction of more hydrogen peroxide to destroy the C-C bonds around the initial defect sites, and a layer-by-layer degradation. The higher the H_2O_2 concentration, the faster the degradation rate. The

1   authors attributed the oxidation power of the hydrogen peroxide to the formation of

2   hydroxyl radicals ($^\bullet$OH) by traces of nickel in the FLG via the Haber–Weiss reaction.

3   Hydroxyl radicals are generated by the Fenton process too. In this well-known method,

4   H_2O_2 is dissociated into $^\bullet$OH under the catalysis of Fe(III) in water, which is reduced to

5   Fe(II). The reaction can be accelerated with external irradiations, such as UV light,

6   giving a photo-Fenton reaction [76-78]. The optimum pH is around $3 - 4$, since at

7   higher pH values, Fe^{3+} precipitates as ferric hydroxide and at lower values, Fe^{3+} forms

8   relatively inactive iron oxohydroxides. It leads to a subsequent neutralization step,

9   where the non-reacted Fe(III) precipitates and produces a tertiary sludge.

10   Zhou et al. [79] mixed 5 mL of an aqueous suspension of 500 mg/L of GO with 20 mL

11   of 20 mmol/L of H_2O_2, and 100 μL of 1.0 mmol/L of $FeCl_3$ in a quartz tube, adjusted

12   the pH to 4 and exposed the vessel to UV radiation (365 nm). Two irradiations powers

13   were tested: 500 and 1000 W. Atomic force microscopy revealed that, with the reaction

14   time increasing, there were more and more holes on the basal plane of GO sheets, and

15   the sizes of the holes became larger. After certain time (higher for 500 W than for 1000

16   W), the nanosheets were fully cut in graphene quantum dots (GQDs), which are

17   graphene sheets with lateral dimensions less of a few nanometers surrounded by oxygen

18   moieties along the edges. The GQDs obtained under 500 and 1000 W for 180 and 15

19   min, respectively, had almost the same dimensions. The decrease in size was

20   accompanied by production of CO_2, decrease of the TOC in the solution and the

21   presence of polyaromatic oxygenated hydrocarbons. For 1000 W and 60 min, the

22   degradation of GO was so high, that no colloidal quantum dots (CQDs) were seen.

23   Additional experiences with RGO showed that this GFN was more slowly oxidised than

1   GO, which led the authors to conclude that $^\bullet$OH mainly attacked hydroxyl and epoxide

2   groups (less abundant in RGO).

3   Bai et al. [80] performed a reaction slower than Zhou et al. [79] in order to obtain CQDs

4   and also to avoid full oxidation of the GO. CQDs are nanomaterials with very

5   interesting electronic and optical properties [1]. They introduced 500 μL of an aqueous

6   solution of 5000 mg/L of GO, 100 μL of 1 mmol/L of $FeCl_3$, and 24.6 mL of nanopure

7   H_2O in the quartz tube, adjusted the pH to 4 with HCl. The vessel was irradiated with a

8   100-W long wave UV light for 3 days. 4.5 μL of 30% H_2O_2 were added each day. The

9   mixture, which was initially dark brown in colour, became lighter and virtually

10 colourless with time. Polyaromatic oxygenated hydrocarbons were identified by

11 electrospray ionization–Fourier transform ion cyclotron resonance, electrospray

12 ionization Orbitrap mass spectrometry, laser desorption ionization time-of-flight mass

13 spectrometry and nuclear magnetic resonance: they had molecular weights between 150

14 and 1000 Da, and were generated on day 1; although after a period of time between day

15 1 and 3, they were no longer prominently present, and the system was dominated by

16 GQDs with a mean diameter of 36 ± 10 nm and thickness ranging from 2 to 5 nm.

17 Feng et al. [81] conducted five conventional Fenton oxidations of ^{14}C-FLG at

18 environmentally realistic concentrations of FLG, Fe^{3+} and H_2O_2 in a 20 mL reaction

19 medium at pH 4 and 25ºC: i) 0.5 mg/L of ^{14}C-FLG, 200 mmol/L of H_2O_2 and 0.05

20 mmol/L of Fe^{3+} for 10 days; ii) 0.02 – 0.5 mg/L of ^{14}C-FLG with 0.1 mmol/L of Fe^{3+}

21 and 2 mmol/L of H_2O_2 for 6 days, iii) 0.2 or 20 mmol/L of H_2O_2 with 0.5 mg/L of ^{14}C-

22 FLG and 0.004 mmol/L of Fe^{3+} for 5 days iv) 0.2 – 200 mmol/L of H_2O_2 with 0.5 mg/L

23 of ^{14}C-FLG and 0.1 mmol/L of Fe^{3+} for 3 days; and v) 0.025 – 0.2 mmol/L of Fe^{3+} with

24 0.5 mg/L of ^{14}C-FLG and 200 mmol/L of H_2O_2 for 3 days. The measured parameters

1 were the amount of $^{14}CO_2$ generated and the remaining mass in solution. In all the

2 experiments, the first one increases with reaction time whereas the second one, falls,

3 and in the first oxidation (i) after 10 days, the residual radioactivity in the reaction

4 solution was below the detection limit, indicating full conversion of the GFN into

5 $^{14}CO_2$. With regard to the concentrations, it was found that in the second oxidation (ii)

6 the higher the ^{14}C-FLG content, the lower the CO_2 production; in the third and fourth

7 Fenton oxidations (iii – iv), the higher the H_2O_2 concentration, the higher the $^{14}CO_2$

8 production and the lower the remaining mass; and in the fifth one (v), $^{14}CO_2$ production

9 went through a maximum and the remaining mass through a minimum at 0.05 mmol/L

10 of Fe^{3+}, due to an excessive concentration of iron ions that can consume the active

11 oxygen species. Transmission electron microscopy and atomic force microscopy

12 revealed that there were holes in the ^{14}C-FLG at day 3, and that the ^{14}C-FLG plane was

13 barely visible at day 5. Liquid chromatography detected high-molecular weight and

14 low-molecular weight secondary products in days 3 and 5, respectively. The 3-day

15 solution was more toxic for *Daphnia magna* than the untreated ^{14}C-FLG suspension,

16 and the aromatics generated displayed less aggregation than the starting nanomaterial.

17 Recently, Zhang et al. [82] subjected a mixture of 200 mL of distilled water and 200 mg

18 of GO at 20ºC to a photo-Fenton reaction by adding an undefined volume of a solution

19 of 1 mg/mL of $FeCl_3$ and 4 mL of H_2O_2, adjusting the pH at 2 and irradiating it with an

20 UV light of wavelength of 185 nm. The brown colour of the solution gradually faded

21 with increasing degradation times. After 28 days, full conversion into CO_2 was

22 obtained. Degradation intermediates of GO at 1, 2, 4, 8, 12, 24 h, 3, 16, 25 and 28 days

23 were determined by UV-vis absorption spectrophotometry, elemental analysis, Fourier

24 transform infrared spectrometry and liquid chromatography-mass spectrometry, and

25 eventually, an oxidation mechanism was proposed.

1   **6. Disinfection**

2   Du et al. [83] are the only ones that studied the effect of some GFNs on the chemical

3   disinfection of water. They prepared suspensions of 10 mg/L GO or RGO in ultrapure

4   water, which were adjusted to pH 7 with 10 mmol/L of phosphate buffer. Next, it was

5   added 10 mg/L of NaClO (as Cl_2) and 2 mg/L of NaBr (in reality, they were synthetic

6   drinking waters with high levels of bromide, not treated wastewaters). In order to

7   compare results, solutions containing 3 mg/L of NOM (as TOC) and 10 m/L of carbon

8   allotropes not belonging to the GFNs (SWNT, MWNT and aminated, hydroxylated and

9   carboxylated forms of the MWNT) were made. After 3 days at 22ºC, the concentrations

10   of the disinfection byproducts formed (as trihalomethanes) were 9.0 µmol/L for NOM,

11   0.95 µmol/L for GO, 0.24 µmol/L for RGO and 0.34-0.51 µmol/L for nanotubes,

12   indicating that either GFNs or non-GFNs had a lower effect on the formation of

13   trihalomethanes in drinking water than NOM. In further experiments, the researchers

14   varied the pH (6 and 8), the bromine concentration (0.5 and 1 mg/L), the chlorine dose

15   (2 and 20 mg/L) and the amount of nanomaterials (5 or 50 mg/L). Generally speaking,

16   alkaline conditions enhance trihalomethanes generation; the lower the concentration of

17   bromine, the lower the by-products content (specially, in the case of GO). The

18   formation of trihalomethanes did not vary significantly with chlorine concentration

19   (except for SWNT and GO, for which it falls very much when decreasing the Cl_2

20   amount) and the higher the nanomaterial content, the lower the concentration of

21   halogenated compounds (except for GO, which follows the opposite trend). A

22   supplementary test with 10 mg/L of GO and 10 mg/L of Cl_2 at pH 7 without NaBr for 5

23   days showed that trihalomethane formation could be fitted to a second-order kinetic.

1   Ozone, another disinfectant, was bubbled for 1 h through a suspension of 500 mg/L of

2   GO in deionised water for 1 h by Gao et al. [84], leading to further oxidation of the

3   GO. Solid-state ^{13}C magic-angle-spinning nuclear magnetic resonance spectroscopy

4   indicated that the content of sp^2-hybridised carbon atoms decreased from 31.5% in the

5   untreated GO to 17.5% after 1h of ozonation. Additionally, annular dark-field scanning

6   transmission electron microscopy revealed a rise in the number of defects (pinholes) in

7   the ozonated species, although the diameter of these pinholes was the same before and

8   after the treatment (around 2.5 nm).

9   UV radiation is also employed for germicidal purposes, and, as referred in section 3, it

10   is able to reduce GO. In fact, photoreduction of GO has been widely studied, because it

11   is considered a green alternative to thermal and chemical techniques [85]. Nonetheless,

12   most of the researchers focus on the design of industrial processes, and therefore, their

13   works deal with systems that lie far from the conditions of wastewater disinfection: non-

14   aqueous suspensions, presence of photocatalysts, wavelengths outside the germicidal

15   range and/or removal of the dissolved oxygen [86-90]. On the other hand, the UV dose,

16   which is the product of the fluence rate (mW/cm^2) and the exposure time (mW/cm^2·s =

17   mJ/cm^2) is always lower than 400 mJ/cm^2 for disinfection [18,91,92], whereas it has to

18   be higher than 9000 mJ/cm^2 to observe photoreduction of GO in purified water for

19   nanomaterial concentrations of 40 – 1200 mg/L [94-96]. The adsorption of Ag$^+$ on the

20   GO sheets [93] or the presence of radical photoinitiators, such as 1 – 3% aryl-alkyl

21   ketone [94], 1% acetone, 2% 2-propanol or a mixture of 1% acetone and 2% 2-

22   propanol [95], decreases the dose required to achieve a specific O:C ratio with regard to

23   purified water alone, and in the case of acetone + 2-propanol, it is almost sure that there

24   is significant photoreduction even around 200 mJ/cm^2. This implies that both the GO

concentration and composition of the tertiary effluent are critical in the attainable level
of reduction during the UV disinfection.

Last but not least, it has to be said that GFNs are able to photocatalytically decompose
aqueous organic pollutants under either UV or visible light, which could lead to a
decrease in the amount of dyes, pesticides, pharmaceuticals and other poorly
biodegradable chemicals in the wastewater. Nonetheless, most of the existing papers on
photodegradation are not centered on GFNs, but on nanocomposites of them with metal
oxides (mainly of TiO_2), thus enhancing the photocatalytic activity of both materials
hanced [90, 96 – 98]. Since these nanocomposites are expected to be widely applied in
the future to water splitting, conversion of CO_2 to valuable hydrocarbons, solar cells and
chemical synthesis [99], a portion of them will probably end in WWTP. Although there
are several good reviews about the photocatalytic decomposition of pollutants by metal
oxide- graphene catalysts [100 – 106], the extent of this decomposition in real sewage is
still unknown, because all the experiments have been performed in monocomponent
solutions so far.

7. Anaerobic treatment of the sludge

As stated in the introduction (section 1), primary and secondary sludges are usually
mixed and digested anaerobically in order to transform the highly putrescible organic
compounds into biogas and into more stable matter. Since sections 3 and 4 indicate that
most of the GFNs will end in the primary and secondary sludges, they will affect the
anaerobic microorganisms. Unfortunately, to the best of our knowledge, no publications
on this subject are available to date. There are three papers that inform on the beneficial
presence of graphenous materials in the removal of nitrogenous aromatic compounds by
anaerobic sludge, but they cannot be extrapolated to the process that takes place in a

1 WWTP, because the bacteria that degrade these pollutants could be more tolerant to the

2 GFNs than those digesting the urban sludge. The studies reported by Colunga et al.

3 [107] showed that 5 mg/L of GO accelerated the reductive biotransformation of the azo

4 dye reactive red 2 during a 72 h test with ethanol + lactate as cosubstrate without

5 decreasing methane production. In the work developed by Wang et al. [108], the

6 degradation of nitrobenzene was performed in presence of glucose, and it was reported

7 that, after 24 h, such degradation was higher for a composite of 100 – 200 mg/L of RGO

8 and anaerobic sludge than for the sludge alone (although the reaction efficiency went

9 through a maximum at 150 mg/L of RGO). Another work by Wang et al. [109], in

10 which it is compared the behaviour of the anaerobic sludge alone and the 150 mg/L of

11 RGO composite for 90 days, concluded that no negative effect of the GFN in the reactor

12 was observed.

13 No negative or positive effects on the anaerobic digestion have been reported for other

14 carbon allotropes, so possible analogies between them and GFN are not available.

15 Nyberg et al. [110] found that concentrations of C_{60} fullerenes up to 30000 mg/(kg dry

16 biomass) did not modify either methane generation or the microbial population during

17 the anaerobic digestion of dead sludge or glucose + ethanol + methanol for more than a

18 month. Li et al. [111] followed up on the degradation of sucrose with 0 or 1000 mg/L of

19 SWNT for 174 h, and indicated that faster substrate consumption and higher amount of

20 methane took place when the nanotubes were added. Yadav et al. [112] incubated the

21 sludge with 0, 1 and 100 mg/L of MWNT for 15 days, and noticed that the higher the

22 nanomaterial concentration, the lower the microbial growth, the cell membrane

23 integrity, the amount of volatile fatty acids generated and the biogas volume.

After the anaerobic treatment, the stabilised biosolids will be landfilled or incinerated, and the GFNs can pass to the soil, to the groundwater or to the air.

8. Conclusions

Graphenous nanomaterials comprise pGr, GO, RGO, FLG and MLG among others, and each form will have a different fate in WWTPs. Generally speaking, pGr, FLG and MLG settle down more easily than RGO in the primary clarifier, whereas GO remains in suspension, although it seems that the addition of a suitable coagulant can remove all the species from the liquid stream. If the oxide passes to the activated sludge process, concentrations of 50 – 1000 mg/L of GO for 3 – 24 h damage the cell membranes, but no studies on the response of microorganisms in more realistic conditions (concentrations of micrograms or nanograms per litre and durations of months/years) have been carried out. GO also affects negatively the anaerobic denitrification, but enhances the anaerobic ammonium oxidation. If the GO to biomass ratio is low, the oxide will be effectively settled in the secondary clarifier. No data on the influence of the nanomaterials in the anaerobic digestion of the primary/secondary sludge are available.

On the other hand, experiments with simple aqueous solutions revealed that several minerals can adsorb GFNs and improve the pretreatment/primary sedimentation. The sunlight, the use of UV radiation and naturally occurring substances can reduce GO to RGO (although there is a work where it is stated that sunlight can oxidise RGO too). Various oxidation techniques, such as hydrogen peroxide, ozone and Fenton oxidise GFNs and could eventually destroy them. Besides, GO and RGO contribute to the formation of trihalomethanes. These tests have to be performed in wastewaters and primary, secondary and tertiary effluents (synthetic or real) in order to use the

1 corresponding results for a better understanding of the fate of graphenous

2 nanomaterials in WWTPs.

9. Acknowledgments

10. Literature cited

9 [1] V. Georgakilas, J.A. Perman, J. Tucek, R. Zboril, Broad family of carbon

10   nanoallotropes: classification, chemistry, and applications of fullerenes, carbon

11   dots, nanotubes, graphene, nanodiamonds, and combined superstructures, Chem.

12   Rev. 115 (2015) 4744-4822.

13 [2] A. Bianco, H.M. Cheng, T. Enoki,, Y. Gogotsi, R.H. Hurt, N. Koratkar, , T.

14   Kyotani, M. Monthioux, C.R. Park, J.M.D. Tascon, J. Zhang, All in the

15   graphene family − a recommended nomenclature for two-dimensional carbon

16   materials, Carbon 65 (2013) 1-6.

17 [3] E.P. Randviir, D.A.C. Brownson, C.E. Banks, A decade of graphene research:

18   production, applications and outlook, Mater. Today 17 (2014) 426-432.

19 [4] K.S. Novoselov, V.I. Falko, L. Colombo, P.R. Gellert, M.G. Schwab, K. Kim, A

20   roadmap for graphene, Nature 490 (2012) 192-200.

21 [5] A.K. Geim, K.S. Novoselov, The rise of graphene, Nat. Mater. 6 (2007) 183-

22   191.

23 [6] D.R. Dreyer,S. Park, C.W. Bielawski, R.S. Ruoff, The chemistry of graphene

24   oxide, Chem. Soc. Rev. 39 (2010) 228-240.

1   [7]   K.E. Whitener Jr, P.E. Sheehan, Graphene synthesis, Diamond. Relat. Mater. 46

2   (2014) 25-34.

3   [8]   C. Soldano, A. Mahmood, E. Dujardin, Production, properties and potential of

4   graphene, Carbon, 48 (2010) 2127-2150.

5   [9]   S. Pei, H.M. Cheng, The reduction of graphene oxide, Carbon 50 (2012) 3210-

6   3228.

7   [10]   R. Arvidsson, D. Kushnir,B.A. Sandén, S. Molander, Prospective life cycle

8   assessment of graphene production by ultrasonication and chemical reduction,

9   Environ. Sci. Technol. 48 (2014) 4529-4536.

10 [11]   D.A.C. Brownson, D.K. Kampouris, C.E. Banks, Graphene electrochemistry:

11   fundamental concepts through to prominent applications, Chem. Soc. Rev. 41

12   (2012) 6944-6976.

13 [12]   K. Yang, B. Xing, Adsorption of organic compounds by carbon nanomaterials in

14   aqueous phase: Polanyi theory and its application, Chem. Rev. 110 (2010) 5989-

15   6008.

16 [13]   K.C. Kemp, H. Seema, M. Saleh, N.H. Le, K. Mahesh, V. Chandra, K.S. Kim,

17   Environmental applications using graphene composites: water remediation and

18   gas adsorption, Nanoscale 5 (2013) 3149-3171.

19 [14]   S.C. Smith, D.F. Rodrigues, Carbon-based nanomaterials for removal of

20   chemical and biological contaminants from water: a review of mechanisms and

21   applications, Carbon 91 (2015) 122-143.

22 [15]   R. Arvidsson, S. Molander, B.A. Sandén, Review of potential environmental and

23   health risks of the nanomaterial graphene, Hum. Ecol. Risk. Asses. 19 (2013)

24   873-887.

1   [16]   A. M. Jastrzebska, A.R. Olszyna, The ecotoxicity of graphene family materials:

2   current status, knowledge gaps and future needs, J. Nanopart. Res. 17 (2015)

3   40/1 - 40/21.

4   [17]   F. Gottschalk, T. Sun, B. Nowack, Environmental concentrations of engineered

5   nanomaterials: review of modeling and analytical studies. Environ. Pollut. 181

6   (2013) 287-300.

7   [18]   Metcalf & Eddy Inc, G. Tchobanoglous, F.L. Burton, H.D. Stensel, Wastewater

8   engineering treatment and reuse, McGraw-Hill Companies Inc, New York,

9   2003.

10   [19]   M.C. Wentzel, Y. Comeau, G.A. Ekama, M.C.M. Van Loosdrecht, D.

11   Brdjanovic, Enhanced biological phosphorus removal, in: M. Henze, M.C.M.

12   van Loosdrecht, G.A. Ekama, D. Brdjanovic (Eds.), Biological wastewater

13   treatment: principles, modelling and design, IWA publishing, London, 2008 pp.

14   155 - 220.

15   [20]   G.A. Ekama, M.C. Wentzel, Nitrogen removal, in: M. Henze, M.C.M. Van

16   Loosdrecht, G.A. Ekama, D. Brdjanovic (Eds.), Biological wastewater

17   treatment: principles, modelling and design, IWA publishing, London, 2008, pp.

18   87 - 138.

19   [21]   L. Appels, J. Baeyens, J. Degrève, R. Dewil, Principles and potential of the

20   anaerobic digestion of waste-activated sludge, Prog. Energy Combust. Sci. 34

21   (2008) 755-781.

22   [22]   I. Chowdhury, M.C. Duch, N.D. Mansukhani, M.C. Hersam, D. Bouchard,

23   Deposition and release of graphene oxide nanomaterials using a quartz crystal

24   microbalance, Environ. Sci. Technol. 48 (2013) 961-969.

1   [23] I. Chowdhury, M.C. Duch, N.D. Mansukhani, M.C. Hersam, D. Bouchard,

2   Interactions of graphene oxide nanomaterials with natural organic matter and

3   metal oxide surfaces, Environ. Sci. Technol. 48 (2014) 9382-9390.

4   [24] Z. Hua, Z. Tang,X. Bai, J. Zhang, L. Yu, H. Cheng, Aggregation and

5   resuspension of graphene oxide in simulated natural surface aquatic

6   environments, Environ. Pollut. 205 (2015) 161-169.

7   [25] K.L. Chen, M. Elimelech, Interaction of fullerene (C60) nanoparticles with silica

8   surfaces coated with humic acid and alginate: measurements,mechanisms, and

9   environmental implications. Environ. Sci. Technol. 42 (2008) 7607–7614

10 [26] K.L. Chen, M. Elimelech, Influence of humic acid on the aggregation kinetics of

11   fullerene (C60) nanoparticles in monovalent and divalent electrolyte solutions, J.

12   Colloid Interface Sci. 309 (2007) 126-134.

13 [27] Y. Zou, X. Wang, Y. Ai, Y. Liu, J. Li, Y. Ji, X. Wang, Coagulation behavior of

14   graphene oxide on nanocrystallined Mg/Al layered double hydroxides: batch

15   experimental and theoretical calculation study, Environ. Sci. Technol. 50 (2016)

16   3658-3667

17 [28] Z. Yang, H. Yan, H. Yang, H. Li,A. Li, R. Cheng, Flocculation performance and

18   mechanism of graphene oxide for removal of various contaminants from water,

19   Water Res. 47 (2013) 3037-3046.

20 [29] J. Zhao, F. Liu, Z. Wang, X. Cao, B. Xing, Heteroaggregation of graphene oxide

21   with minerals in aqueous phase, Environ. Sci. Technol. 49 (2015) 2849-2857.

22 [30] G. Huang, H. Guo, J. Zhao, Y. Liu, B. Xing, Effect of co-existing kaolinite and

23   goethite on the aggregation of graphene oxide in the aquatic environment, Water

24   Res. 102 (2016) 313-320.

1   [31] X. Ren, J. Li, X. Tan, W. Shi, C. Chen, D. Shao, T. Wen, L. Wang, G. Zhao, G.

2   Sheng, X. Wang, Impact of Al2O3 on the aggregation and deposition of

3   graphene oxide, Environ. Sci. Technol. 48 (2014) 5493-5500.

4   [32] W.C. Hou, I. Chowdhury, D.G. Goodwin, W.M. Henderson, D.H. Fairbrother,

5   D. Bouchard, R.G. Zepp, Photochemical transformation of graphene oxide in

6   sunlight, Environ. Sci. Technol. 49 (2015) 3435-3443.

7   [33] M. Agharkar, S. Kochrekar, S. Hidouri, M.A. Azeez, Trends in green reduction

8   of graphene oxides, issues and challenges: a review, Mater. Res. Bull. 59 (2015)

9   323-328.

10 [34] S. Thakur, N. Karak, Alternative methods and nature-based reagents for the

11   reduction of graphene oxide: A review, Carbon 94 (2015) 224-242.

12 [35] H. Fu, X. Qu, W. Chen, D. Zhu, Transformation and destabilization of graphene

13   oxide in reducing aqueous solutions containing sulfide, Environ. Toxicol. Chem.

14   33 (2014) 2647-2653.

15 [36] F. Wang, F. Wang, G. Gao, W. Chen, Transformation of graphene oxide by

16   ferrous iron: environmental implications, Environ. Toxicol. Chem. 34 (2015)

17   1975-1982.

18 [37] I. Chowdhury, W.C. Hou, D. Goodwin, M. Henderson, R.G. Zepp, D. Bouchard,

19   Sunlight affects aggregation and deposition of graphene oxide in the aquatic

20   environment, Water Res. 78 (2015) 37-46.

21 [38] J. Texter, Graphene dispersions, Curr. Opin. Colloid Interface Sci. 19 (2014)

22   163-174.

23 [39] W. Fan, X. Jiang, Y. Lu, M. Huo, S. Lin, Z. Geng, Effects of surfactants on

24   graphene oxide nanoparticles transport in saturated porous media, J. Environ.

25   Sci. 35 (2015) 12-19.

1 [40] I. Chowdhury, M.C. Duch, N.D. Mansukhani, M.C. Hersam, D. Bouchard,

2   Colloidal properties and stability of graphene oxide nanomaterials in the aquatic

3   environment, Environ. Sci. Technol. 47 (2013) 6288-6296.

4 [41] I. Chowdhury, N.D. Mansukhani, L.M. Guiney, M.C. Hersam, D. Bouchard,

5   Aggregation and stability of reduced graphene oxide: complex roles of divalent

6   cations, ph, and natural organic matter, Environ. Sci. Technol. 49 (2015) 10886-

7   1089

8 [42] L. Wu, L. Liu, B. Gao, R. Muñoz-Carpena, M. Zhang, H. Chen, Z. Zhou, H.

9   Wang, Aggregation kinetics of graphene oxides in aqueous solutions:

10   experiments, mechanisms, and modeling, Langmuir 29 (2013) 15174-15181.

11 [43] N.S. Andryushina, O.L. Stroyuk, I.B. Yanchuk, A.V. Yefanov, A dynamic light

12   scattering study of photochemically reduced colloidal graphene oxide, Colloid.

13   Polym. Sci. 292 (2014) 539-546.

14 [44] X. Hu, M. Zhou, Q. Zhou, Ambient water and visible-light irradiation drive

15   changes in graphene morphology, structure, surface chemistry, aggregation, and

16   toxicity, Environ. Sci. Technol. 49 (2015) 3410-3418.

17 [45] Z. Wang, Y. Gao, S. Wang, H. Fang, D. Xu, F. Zhang, Impacts of low-

18   molecular-weight organic acids on aquatic behavior of graphene nanoplatelets

19   and their induced algal toxicity and antioxidant capacity Environ. Sci. Pollut.

20   Res. 23 (2016) 10938-10945.

21 [46] T. Jiao, H. Zhao, J. Zhou, Q. Zhang, X. Luo, J. Hu, Q. Peng, X. Yan, Self-

22   assembly reduced graphene oxide nanosheet hydrogel fabrication by anchorage

23   of chitosan/silver and its potential efficient application toward dye degradation

24   for wastewater treatments, ACS Sustainable Chem. Eng. 3 (2015) 3130 – 3139.

1   [47]   T. Jiao, H. Guo, Q. Zhang, Q. Peng, Y. Tang, X. Yan, B. Li, Reduced graphene

2   oxide-based silver nanoparticle-containing composite hydrogel as highly

3   efficient dye catalysts for wastewater treatment, Sci. Rep. 5 (2015) 11873.

4   [48]   T. Jiao, Y. Liu, Y. Wu, Q. Zhang, X. Yan, F. Gao, A.J.P. Bauer, J. Liu, T. Zeng,

5   B. Li, Facile and scalable preparation of graphene oxide-based magnetic hybrids

6   for fast and highly efficient removal of organic dyes, Sci. Rep. 5 (2015) 12451.

7   [49]   Z. Hua, J. Zhang, X. Bai, Z. Ye, Z. Tang, L. Liang, Y. Liu, Aggregation of

8   TiO2–graphene nanocomposites in aqueous environment: Influence of

9   environmental factors and UV irradiation, Sci. Total Environ. 539 (2016) 196-

10   205.

11   [50]   J. Liu, P. Li, H. Xiao, Y. Zhang, X. Shi, X. Lü, X. Chen, Understanding

12   flocculation mechanism of graphene oxide for organic dyes from water:

13   experimental and molecular dynamics simulation, AIP Adv. 5 (2015) 117-151.

14   [51]   H.M. Hegab, A. ElMekawy, L. Zou, D. Mulcahy, C.P. Saint, M. Ginic-

15   Markovic, The controversial antibacterial activity of graphene-based materials,

16   Carbon 105 (2016) 362-376.

17   [52]   O.N. Ruiz, K.A.S. Fernando, B. Wang, N.A. Brown, P.G. Luo, N.D. McNamara

18   , M. Vangsness, Y.P. Sun, C.E. Bunker, Graphene oxide: a nonspecific enhancer

19   of cellular growth, ACS Nano 5 (2011) 8100-8107.

20   [53]   F. Ahmed, D.F. Rodrigues, Investigation of acute effects of graphene oxide on

21   wastewater microbial community: a case study, J. Hazard. Mater. 256–257

22   (2013) 33-39.

23   [54]   R.G. Combarros, S. Collado, M. Díaz, Toxicity of graphene oxide on growth

24   and metabolism of Pseudomonas putida, J. Hazard. Mater. 310 (2016) 246-252.

1   [55]   Y. Yang, Z. Yu, T. Nosaka, K. Doudrick, K. Hristovski, P. Herckes, P.

2   Westerhoff, Interaction of carbonaceous nanomaterials with wastewater

3   biomass, Front. Environ. Sci. Eng. 9 (2015) 823-831.

4   [56]   M. Ali, S. Okabe, Anammox-based technologies for nitrogen removal: advances

5   in process start-up and remaining issues, Chemosphere 141 (2015) 144-153.

6   [57]   B. Ma, S. Wang, S. Cao, Y. Miao, F. Jia, R. Du, Y. Peng, Biological nitrogen

7   removal from sewage via anammox: recent advances, Bioresour. Technol. 200

8   (2016) 981-990.

9   [58]   S. Ghafari, M. Hasan, M.K. Aroua, Bio-electrochemical removal of nitrate from

10   water and wastewater—a review, Bioresour. Technol. 99 (2008) 3965-3974.

11   [59]   S. Lackner, E.M. Gilbert, S.E. Vlaeminck, A. Joss, H. Horn, M.C.M. van

12   Loosdrecht, Full-scale partial nitritation/anammox experiences − an application

13   survey, Water Res. 55 (2014) 292-303.

14   [60]   H. Gao, Y.D. Scherson, G.F. Wells, Towards energy neutral wastewater

15   treatment: methodology and state of the art, Environ. Sci. Proc. Imp. 16 (2014)

16   1223-1246.

17   [61]   D. Wang, G. Wang, G. Zhang, X. Xu, F. Yang, F Using graphene oxide to

18   enhance the activity of anammox bacteria for nitrogen removal, Bioresour.

19   Technol. 131 (2013) 527-530.

20   [62]   G. Wang, X. Xu, F. Yang, H. Zhang, D. Wang, Using graphene oxide to

21   reactivate the anaerobic ammonium oxidizers after long-term storage, J.

22   Environ. Chem. Eng. 2 (2014) 974-980.

23   [63]   X. Yin, S. Qiao, C. Yu, T. Tian, J. Zhou, Effects of reduced graphene oxide on

24   the activities of anammox biomass and key enzymes, Chem. Eng. J. 276 (2015)

25   106-112.

1   [64]   X. Yin, S. Qiao, J. Zhou, X. Tang, Fast start-up of the anammox process with

2   addition of reduced graphene oxides, Chem. Eng. J. 283 (2016) 160-166.

3   [65]   D. Chen, X. Wang, K. Yang, H. Wang, Response of a three dimensional

4   bioelectrochemical denitrification system to the long-term presence of graphene

5   oxide, Bioresour. Technol. 214 (2016) 24-29.

6   [66]   S. Chowdhury, R. Balasubramanian, Recent advances in the use of graphene-

7   family nanoadsorbents for removal of toxic pollutants from wastewater, Adv.

8   Colloid Interface Sci. 204 (2014) 35 – 56.

9   [67]   S.C. Smith, F. Ahmed, K.M. Gutierrez, D.F. Rodrigues, A comparative study of

10   lysozyme adsorption with graphene, graphene oxide, and single-walled carbon

11   nanotubes: potential environmental applications, Chem. Eng. J. 240 (2014) 147

12   – 154.

13   [68]   J. Wang, B. Chen, Adsorption and coadsorption of organic pollutants and a

14   heavy metal by graphene oxide and reduced graphene materials, Chem. Eng. J.

15   281 (2015) 379 – 388.

16   [69]   Y. Zhou, O. G. Apul, T. Karanfil, Adsorption of halogenated aliphatic

17   contaminants by graphene nanomaterials, Water Res. 79 (2015) 57 – 67.

18   [70]   J. Zhao, Z. Wang, J.C. White, B. Xing, Graphene in the aquatic environment:

19   adsorption, dispersion, toxicity and transformation, Environ. Sci. Technol. 48

20   (2014) 9995-10009.

21   [71]   K.A. Third, A.O. Sliekers, J.G. Kuenen, M.S.M. Jetten, The CANON system

22   (Completely Autotrophic Nitrogen-removal Over Nitrite) under ammonium

23   limitation: interaction and competition between three groups of bacteria, Syst.

24   Appl. Microbiol. 24 (2001) 588-596.

1   [72]   A.A. van de Graaf, P. de Bruijn, L.A. Robertson, M.S.M. Jetten, J.G. Kuenen,

2   Autotrophic growth of anaerobic ammonium-oxidizing micro-organisms in a

3   fluidized bed reactor, Microbiology 142 (1996) 2187-2196.

4   [73]   Y. Li, F. Yu, W. He, W. Yang, The preparation and catalytic performance of

5   graphene-reinforced ion-exchange resins RSC Advances 5 (2015) 2550-2561.

6   [74]   A. Aghigh, V. Alizadeh, H.Y. Wong, M. Shabiul Islam, N. Amin, M. Zaman,

7   Recent advances in utilization of graphene for filtration and desalination of

8   water: a review, Desalination 365 (2015) 389 - 397.

9   [75]   W. Xing, G. Lalwani, I. Rusakova, B. Sitharaman, Degradation of graphene by

10   hydrogen peroxide, Part. Part. Syst. Char. 31 (2014) 745-750.

11 [76]   A. Babuponnusami, K. Muthukumar, A review on Fenton and improvements to

12   the Fenton process for wastewater treatment, J. Environ. Chem. Eng. 2 (2014)

13   557-572.

14 [77]   G. Pliego, J.A. Zazo, P. Garcia-Muñoz, M. Munoz, J.A. Casas, J.J. Rodriguez,

15   Trends in the intensification of the Fenton process for wastewater treatment: an

16   overview, Crit. Rev. Environ. Sci. Technol. 45 (2015) 2611-2692.

17 [78]   N. Wang, T. Zheng, G. Zhang, P. Wang, A review on Fenton-like processes for

18   organic wastewater treatment, J. Environ. Chem. Eng. 4 (2016) 762-787.

19 [79]   X. Zhou, Y. Zhang, C. Wang, X. Wu, Y. Yang, B. Zheng, H. Wu, S. Guo, J.

20   Zhang, Photo-Fenton reaction of graphene oxide: a new strategy to prepare

21   graphene quantum dots for DNA cleavage, ACS Nano 6 (2012) 6592-6599.

22 [80]   H. Bai, W. Jiang, G.P. Kotchey, W.A. Saidi, B.J. Bythell, J.M. Jarvis, A.G.

23   Marshall, R.A.S. Robinson, A. Star, Insight into the mechanism of graphene

24   oxide degradation via the photo-Fenton reaction, J. Phys. Chem. C. 118 (2014)

25   10519-10529.

1   [81]   Y. Feng, K. Lu, L. Mao, X. Guo, S. Gao, E.J. Petersen, Degradation of 14C-

2   labeled few layer graphene via Fenton reaction: Reaction rates, characterization

3   of reaction products, and potential ecological effects, Water Res. 84 (2015) 49-

4   57.

5   [82]   C.Z. Zhang, T. Li, Y. Yuan, J. Xu, An efficient and environment-friendly

6   method of removing graphene oxide in wastewater and its degradation

7   mechanisms, Chemosphere 153 (2016) 531-540.

8   [83]   T. Du, Y. Wang, X. Yang, W. Wang, H. Guo, X. Xiong, R. Gao, X. Wuli, A.S.

9   Adeleye, Y. Li, Mechanisms and kinetics study on the trihalomethanes

10   formation with carbon nanoparticle precursors, Chemosphere 154 (2016) 391-

11   397.

12   [84]   W. Gao, G. Wu, M.T. Janicke, D.A. Cullen, R. Mukundan, J.K. Baldwin, E.L.

13   Brosha, C. Galande, P.M. Ajayan, K.L. More, A.M. Dattelbaum, P. Zelenay,

14   Ozonated graphene oxide film as a proton-exchange membrane, Angewandte

15   Commun. 53 (2014) 3588 - 3593.

16   [85]   Y.L. Zhang, L. Guo, H. Xia, Q.D. Chen, J. Feng, H.B. Sun, Photoreduction of

17   graphene oxides: methods, properties, and applications, Adv. Opt. Mater. 2

18   (2014) 10 - 28.

19   [86]   O. Akhavan, Photocatalytic reduction of graphene oxides hybridized by ZnO

20   nanoparticles in ethanol, Carbon 49 (2011) 11 - 18.

21   [87]   H. Li, S. Pang, X. Feng, K. Müllen, C. Bubeck, Polyoxometalate assisted

22   photoreduction of graphene oxide and its nanocomposite formation, Chem.

23   Commun. 46 (2010) 6243 - 6245.

1   [88]   H. Li, H., S. Pang, S. Wu, X. Feng, K. Müllen, C. Bubeck, Layer-by-layer

2   assembly and UV photoreduction of graphene polyoxometalate composite films

3   for electronics, J. Am. Chem. Soc. 133 (2011) 9423 - 9429.

4   [89]   Y.H. Ding, P. Zhang, Q. Zhuo, H.M. Ren, Z.M. Yang, Y. Jiang, A green

5   approach to the synthesis of reduced graphene oxide nanosheets under UV

6   irradiation, Nanotechnology 22 (2011) 215601/1 - 215601/5.

7   [90]   L. Guardia, S. Villar-Rodil, J.I. Paredes, R. Rozada, A. Martínez-Alonso, J.M.D.

8   Tascon, UV light exposure of aqueous graphene oxide suspensions to promote

9   their direct reduction, formation of graphene–metal nanoparticle hybrids and dye

10   degradation, Carbon 50 (2012) 1014 - 1024.

11   [91]   W.A.M. Hijnen, E.F. Beerendonk, G.J. Medema, Inactivation credit of UV

12   radiation for viruses, bacteria and protozoan (oo)cysts in water: A review, Water

13   Res. 40 (2016) 3 - 22.

14   [92]   K. Song, M. Mohseni, F. Taghipour, Application of ultraviolet light-emitting

15   diodes (UV-LEDs) for water disinfection: a review, Water Res. 94 (2016) 341 -

16   349.

17   [93]   Y. Matsumoto, M. Koinuma, S.Y. Kim, Y. Watanabe, T. Taniguchi, K.

18   Hatakeyama, H. Tateishi, S. Ida, Simple photoreduction of graphene oxide

19   nanosheet under mild conditions, ACS Appl. Mater. Interfaces 2 (2010) 3461-

20   3466.

21   [94]   P. Fabbri, L. Valentini, S. Bittolo Bon, D. Foix, L. Pasquali, M. Montecchi, In-

22   situ graphene oxide reduction during UV-photopolymerization of graphene

23   oxide/acrylic resins mixtures, Polymer 53 (2012) 6039 - 6044.

24   [95]   R. Flyunt, W. Knolle, A. Kahnt, C.E. Halbig, A. Lotnyk, T. Haupl, A. Prager, S.

25   Eigler, B. Abel, High quality reduced graphene oxide flakes by fast kinetically

1   controlled and clean indirect UV-induced radical reduction, Nanoscale 8 (2016)

2   7572 - 7579.

3   [96]   Z. Xiong, L.L. Zhang, J. Ma, X.S. Zhao, Photocatalytic degradation of dyes over

4   graphene–gold nanocomposites under visible light irradiation, Chem. Commun.

5   46 (2010) 6099 – 6101.

6   [97]   J. Zhang, Z. Xiong, X.S. Zhao, Graphene–metal–oxide composites for the

7   degradation of dyes under visible light irradiation, J. Mater. Chem. 21 (2011)

8   3634 – 3640.

9   [98]   C.-C. Fu, R.-S. Juang, M.M. Huq, C.-T. Hsieh, Enhanced adsorption and

10   photodegradation of phenol in aqueous suspensions of titania/graphene oxide

11   composite catalysts, J. Taiwan Inst. Chem. Eng. 67 (2016) 338 – 345.

12   [99]   D. Chen, H. Zhang, Y. Liu, J. Li, Graphene and its derivatives for the

13   development of solar cells, photoelectrochemical, and photocatalytic

14   applications, Energy Environ. Sci. 6 (2013) 1362 – 1387.

15   [100]   X. An, J.C. Yu, Graphene-based photocatalytic composites, RSC Advances 1

16   (2011) 1426- 1434.

17   [101]   L. Han, P. Wang, S. Dong, Progress in graphene-based photoactive

18   nanocomposites as a promising class of photocatalyst, Nanoscale 4 (2012) 5814

19   – 5825.

20   [102]   S. Morales-Torres, L. M. Pastrana-Martínez, J.L. Figuereido, J.L. Faria, A.M.T.

21   Silva, Design of graphene-based TiO_2 photocatalysts-a review, Environ. Sci.

22   Pollut. Res. 19 (2012) 3676 – 3687.

23   [103]   L.-L. Tan, S.-P. Chai, A.R. Mohamed, Synthesis and applications of graphene-

24   based TiO_2 photocatalysts, ChemSusChem. 5 (2012) 1868 – 1882.

[104] Q. Xiang, J. Yu, M. Jaroniec, Graphene-based semiconductor photocatalysts, Chem. Sooc. Rev. 41 (2012) 782 – 796.

[105] N. Zhang, Y. Zhang, Y.-J. Xu, Recent progress on graphene-based photocatalysts: current status and future perspectives, Nanoscale 4 (2012) 5792 – 5813.

[106] B. Luo, G. Liu, L. Wang, Recent advances in 2D materials for photocatalysis, Nanoscale 8 (2016) 6904 – 6920.

[107] A. Colunga, J.R. Rangel-Mendez, L.B. Celis, F.J. Cervantes, Graphene oxide as electron shuttle for increased redox conversion of contaminants under methanogenic and sulfate-reducing conditions, Bioresour. Technol. 175 (2015) 309 - 314.

[108] J. Wang, D. Wang, D., G. Liu, R. Jin, H. Lu, Enhanced nitrobenzene biotransformation by graphene-anaerobic sludge composite, J. Chem. Technol. Biotechnol. 89 (2014) 750 - 755.

[109] J. Wang, H. Zhang, D. Wang, H. Lu, J. Zhou, Effect of bioreduced graphene oxide on anaerobic biotransformation of nitrobenzene in an anaerobic reactor, Environ. Technol. 37 (2016) 39-45.

[110] L. Nyberg, R.F. Turco, L. Nies, Assessing the impact of nanomaterials on anaerobic microbial communities, Environ. Sci. Technol. 42 (2008) 1938-1943.

[111] L.L. Li, Z.H. Tong,C.Y. Fang, J. Chu, H.Q. Yu, Response of anaerobic granular sludge to single-wall carbon nanotube exposure, Water Res. 70 (2015) 1-8.

[112] T. Yadav, A.A. Mungray, A.K. Mungray, Effect of multiwalled carbon nanotubes on UASB microbial consortium, Environ. Sci. Pollut. Res. 23 (2016) 4063-4072.

Tables

Table 1. Published literature dealing with GFNs in activated sludge.

REFERENCE	MATERIALS	TESTS AND MEASUREMENTS	RESULTS
[53].	• Activated sludge from Sims South Bayou WWTP (Houston, TX), with 2666.6 mg/L of TSS, 9.81 mg/L of DO, 1.46 mg/L of NH_3-N, 5.3 of mg/L PO_4^{3-} and pH 7.3. • Concentrations of 0, 10, 20, 50, 100, 200 and 300 mg/L GO.	• Incubation of GO and activated sludge for 5 h before measuring microbial metabolic activity, bacterial viability, biodegradation of organic carbon, dewaterability after settling and turbidity of the supernatant by C_{12}-resofurin fluorescence, plate counting, BOD_5, capillary suction time and nephelometry, respectively. Scanning electron microscopy and fluorescence imaging were also carried out to see the interaction of GO with the sludge flocs. • Incubation of GO and activated sludge for 20 h before determining the amounts of ammonia and phosphate by colourimetry. • Quantification of the ROS generated by each GO concentration through the Ellman's assay, based in the oxidation of glutathione.	• The higher the GO concentration, the lower the metabolic activity. • The BOD_5 decrease was the same for the six concentrations tested (around 50% of that obtained at 0 mg/L). • Bacterial viability, NH_3-N, NO_3-N and capillary suction time were only affected in the range 50 – 300 mg/L GO, whereas changes in turbidity were important for 100 – 300 mg/L GO. Alterations of PO_4^{3-} and ROS generation were statistically significant for 200 – 300 mg/L GO. Bacterial viability and NO_3-N decreased, but NH_3-N, PO_4^{3-}, ROS generation, capillary suction time and turbidity became higher. • Fluorescence images showed that GO was accumulated inside the sludge flocs, and scanning electron microscopy revealed adsorption of bacteria and other microorganisms onto the GO sheets.

Table 1. Published literature dealing with GFNs in activated sludge (continuation).

REFERENCE	MATERIALS	TESTS AND MEASUREMENTS	RESULTS
[54].	• Pure culture of *Pseudomonas putida* (bacteria predominant in activated sludge) in synthetic urban wastewater. • The urban sewage was composed of 5 g/L of peptone, 3 g/L of beef, 0.422 g/L of KH_2PO_4, 0.375 g/L of K_2HPO_4, 0.244 g/L of $(NH_4)_2SO_4$, 0.05 g/L of $MgSO_4·7H_2O$, 0.054 g/L of $C_6H_{11}FeNO_7$, 0.015 g/L of $CaCl_2·2H_2O$ and 0.015 g/L of NaCl. • Concentrations of 0, 50, 100, 250, 500 and 1000 mg/L GO.	• GO-bacteria contact time of 0, 3, 6, 8, 11 and 24 h at 30ºC and 200 rpm. • Bacterial growth was measured by optical density, plate counting and flow cytometry. The percentages of viable, dead and damaged cells were obtained through a multiparametric flow cytometry method based on a dual propidium iodide/ carboxyfluoresceindiacetate staining.	• The higher the GO concentration, the lower the optical densities, but the fall was not linear. The decrease from 0 to 50 mg/L was much more important than from 50 to 100 mg/L. At 1000 mg/L the optical density was almost zero for all the times. The results obtained using flow cytometry were more disperse, but corroborate these findings. Multiparametric cytometry revealed that the percentage of viable cells went through a maximum with time at 6 h for GO concentrations of 0 – 250 mg/L, but went through a minimum at 11 h for 500 – 1000 mg/L GO. Additionally, the percentage of dead cells barely increased, indicating that viable cells tend to become into damaged cells.

Table 1. Published literature dealing with GFNs in activated sludge (continuation).

REFERENCE	MATERIALS	TESTS AND MEASUREMENTS	RESULTS
[54].	• Pure culture of *Pseudomonas putida* (bacteria predominant in activated sludge) in synthetic industrial wastewater. • The industrial sewage contained 0.5 g/L of K_2HPO_4, 0.3 g/L of $(NH_4)_2SO_4$, 0.05 g/L of $MgSO_4 \cdot 7H_2O$, 0.01 g/L of $FeCl_3 \cdot 6H_2O$, 0.01 g/L of $CaCl_2 \cdot 2H_2O$, 0.05 g/L of tryptone, 500 mg/L of salicylic acid and 10 mL/L of trace solution (composed of 8 mg/L of $ZnSO_4 \cdot 7H_2O$, 4 mg/L of H_3BO_3, 4 mg/L of $Na_2MoO_4 \cdot 2H_2O$, 4 mg/L of $CuSO_4 \cdot 5H_2O$, 4 mg/L of $MnCl_2 \cdot 4H_2O$ and 4 mg/L of $CoCl_2 \cdot 6H_2O$) • Concentrations of 0, 50, 100, 250, 500 and 1000 mg/L GO.	• GO-bacteria contact time of 0, 3, 6, 8, 11 and 24 h at 30ºC and 250 rpm. • Bacterial growth was measured by optical density, plate counting and flow cytometry. The percentages of viable, dead and damaged cells were obtained through a multiparametric flow cytometry method based on a dual propidium iodide/ carboxyfluoresceindi-acetate staining. • An aqueous suspension of GO, a *P. putida* culture in absence of GO and the *P. putida* culture in the industrial sewage with 100 mg/L of GO after 11 h were examined by scanning electron microscopy.	• The concentration of salicylic acid decreased with time thanks to the ability of *P. putida* to degrade it. Inhibition slightly increased with GO concentration, but it was only important at 1000 mg/L of GO. Bacterial growth, determined by optical density and plate counting, is similar to that measured in urban sewage by optical density and flow cytometry, respectively, but the growth was less intense (due to the higher availability of carbon and nitrogen sources in the urban wastewater) and data were more disperse. Multiparametric cytometry revealed that the negative effect of GO on viability becomes important for concentrations of 100 mg/L or higher. For 250 – 1000 mg/L GO the viability percentages rapidly decreased during the first 3 h, achieving final values around 20%. In all the experiments, the percentages of dead cells remained approximately constant, indicating that viable cells tend to become into damaged cells. • Scanning electron micrograph showed that, in absence of GO, bacteria had smooth and flawless outer membranes, but in presence of GO, they showed a rough surface, probably because of the damage (attributed to the GO edges).

Table 1. Published literature dealing with GFNs in activated sludge (continuation).

REFERENCE	MATERIALS	TESTS AND MEASUREMENTS	RESULTS
[55].	- Activated sludge (from laboratory scale SBR) in a 1 mM of $NaHCO_3$ buffer solution with pH adjusted to 7. 25 mg/L of GO and 25 mg/L of oxidised MWNTs mixed with sludge containing 50 – 3000 mg/L of TSS. 0.3 – 8.3 mg/L of FLG mixed with sludge containing 50 mg/L of TSS, because the analytical technique did not allow to study the same conditions than GO and oxidised MWNT.	- Mixing of nanomaterials and biomass for 3 h, followed by 30 min of gravity settling. Control tests without sludge were carried out to determine how much removal was due to aggregation of the nanomaterial. - Oxidised MWNTs and GO were quantified using UV-Vis light scattering spectrophotometry in the supernatant, whereas FLG was determined by programmed thermal analysis in settled biomass.	- Oxidised MWNTs were nearly completely removed without biomass by aggregation and sedimentation. Sludge did not stabilise the nanomaterial suspension, and removals greater than 96% were obtained in all the cases. - GO did not undergo sedimentation without biomass. After addition of sludge and sedimentation, removals varied from 10% at 50 mg/L of TSS to almost 100% at 3000 mg/L of TSS. The amount of GO in the biomass and its concentration in the liquid could be related by $q=5.0\ C_L^{0.5}$ - FLG did not settle without biomass. After addition of sludge and sedimentation, the removals were around 11% for all the FLG concentrations tested, and $q=2.2\ C_L^{1.1}$. The Freundlich model allowed extrapolation to 25 mg/L of FLG and 50 – 3000 mg/L of TSS.

Table 2. Published literature related to GFNs and autotrophic removal of inorganic nitrogen.

REFERENCE	MATERIALS	TESTS AND MEASUREMENTS	RESULTS
[61].	• Serum bottles with 100 mL of synthetic wastewater and 350 mg/L of VSS. Bacteria belonged to *Candidatus Brocadia anammoxidans*. • Apart from 120 mg/L of NH_4-N and 150 mg/L of NO_2-N, the synthetic wastewater consisted of [61]: 1.25 g/L of $KHCO_3$, 0.025 g/L of KH_2PO_4, 0.3 g/L of $CaCl_2 \cdot 2H_2O$, 0.2 g/L of $MgSO_4 \cdot 7H_2O$, 0.00625 g/L $FeSO_4$, 0.00625 g/L EDTA and 1.25 mL/L of trace elements solution. This trace element solution contained 15 g/L of EDTA, 0.43 g/L of $ZnSO_4 \cdot 7H_2O$, 0.24 g/L of $CoCl_2 \cdot 6H_2O$, 0.99 g/L of $MnCl_2 \cdot 4H_2O$, 0.25 g/L of $CuSO_4 \cdot 5H_2O$, 0.22 mg/L of $NaMoO_4 \cdot 2H_2O$, 0.19 g/L of $NiCl_2 \cdot 6H_2O$, 0.21 g/L of $NaSeO_4 \cdot 10H_2O$, 0.014 g/L H_3BO_4 and 0.05 g/L $NaWO_4 \cdot 2H_2O$. • 0, 50, 100 and 150 mg/L GO.	• Contact times of 7, 14, 21, 28, 35 and 42 h at 35ºC and 150 rpm. Absence of O_2. Protection from light. • Ammonia, nitrites and nitrates were measured colourimetrically. • EPS were extracted by cation exchange. Their carbohydrate fraction was determined by the anthrone method and their protein content by the Lowry technique. • Bacterial morphology was carried out by transmission electron microscopy.	• For a given GO concentration, NH_4-N and NO_2-N in the mineral medium decreased monotonically with increasing time, whereas NO_3-N (which was absent in the mineral medium) increased. • For a given contact time, NH_4-N and NO_2-N went through a minimum with GO concentration, whereas NO_3-N went through a maximum. These results correspond to 100 mg/L GO. • After 42 h, the concentrations of both proteins and carbohydrates in the EPS went through a maximum at 100 mg/L GO. For all the concentrations (even 0 mg/L) proteins were more abundant than carbohydrates • Transmission electron microscopy for a sample with 100 mg/L GO revealed that bacteria were packed and supported by the graphene nanosheets, which acted as scaffolds for cell attachment and favoured the aggregation of anammox bacteria.

5

Table 2. Published literature related to GFNs and autotrophic removal of inorganic nitrogen (continuation).

REFERENCE	MATERIALS	TESTS AND MEASUREMENTS	RESULTS
[62].	• Three sludges (A, B and C) from an anammox reactor, stored for 2 months with proper concentration of nutrients. • Synthetic wastewater with 1250 mg/L of $KHCO_3$, 25 mg/L of KH_2PO_4, 200 mg/L of $MgSO_4 \cdot 7H_2O$ 300 mg/L of $CaCl_2$, 18.75 mg/L of $FeSO_4 \cdot 7H_2O$, 6.25 mg/L of EDTA and variable concentration of NH_4-N (21.6 – 300 mg/L) and NO_2-N (28.4 – 400 mg/L), but with a NO_2-N to NH_4-N molar ratio around 1.3 • Sludge A was stored at room temperature without GO, sludge B was stored at 4ºC without GO and sludge C was stored at 4ºC with 100 mg/L GO.	• After the storage, the sludges were put in three up-flow reactors, covered with a black vinyl sheet enclosure to protect bacteria from light. Wastewater was deoxygenated and pumped at 0.75 L/h during 6 weeks. Temperature and pH were set to 35ºC and 7.5, respectively. • NH_4-N and NO_2-N were measured colourimetrically, NO_3-N by chromatography, VSS by weighing after drying and burning, the sludge volume index (SVI, a estimation of the sedimentation performance) was gauged in a 100 mL graduated cylinder with settling for 30 min and EPS were extracted by cation exchange and analysed in terms of proteins and carbohydrates. • Morphology, particle size of the sludge granules, specific anammox activity and microbial populations were evaluated by a scanning electron microscope, a laser analyser, production of N_2 and fluorescence in situ hybridization, respectively.	• Total nitrogen removal rate followed the decreasing order sludge C > sludge B > sludge A. • VSS went through a tiny minimum with reaction time at 2 weeks. Sludge C always display higher VSS than sludge B, sludge A being the sludge with lowest amount of volatile solids. • The higher the reaction time, the lower the SVI and the amount of EPS. At a constant time, both parameters were higher in sludge A than in the other two sludges. • The decline of EPS and the minimum of VSS was attributed to the fact that the sludge with poor settling properties (high SVI) was washed out. • Scanning electron microscopy on day 31 revealed that microorganisms were mostly elliptical, forming spherical bacterial clusters with rough surface. The clusters were bonded together by some sticky membranous substance (allegedly, the EPS). Additionally, no damage of the cell membrane by the sharp edges of the GO nanosheets was observed. • The initial particle sizes were in all cases about 90 μm and eventually increased to 153, 189 and 230 μm for sludges A, B and C, respectively. • Specific anammox activites for sludges A, B and C were 0.30, 0.42 and 0.44 g / (g VSS·day), respectively. • Anammox bacteria were the dominant population in sludge C on day 27, but there were other bacteria as ammonia-oxidising bacteria, denitrifying bacteria and so on. Allegedly, a small amount of ammonia-oxidising bacteria can keep anaerobic conditions by consuming oxygen that leaks into the system, cell lysis products and metabolic products.

Table 2. Published literature related to GFNs and autotrophic removal of inorganic nitrogen (continuation).

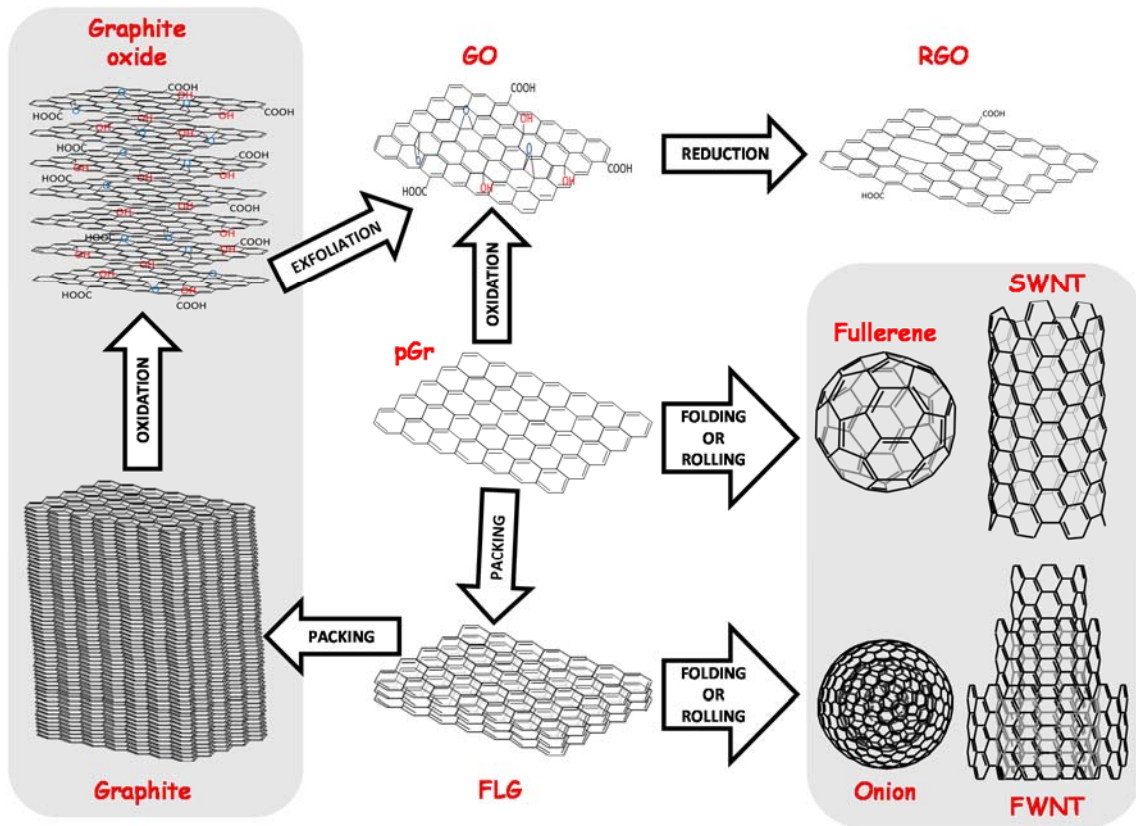| REFERENCE	MATERIALS	TESTS AND MEASUREMENTS	RESULTS
[63].	• Serum bottles with 100 mL of synthetic wastewater and 2020 mg/L of VSS. Anammox bacteria of KSU-1 strain. • Apart from 65 mg/L of NH_4-N and 95 mg/L of NO_2-N, the wastewater contained [62]: 500 mg/L of $KHCO_3$, 27.2 of mg/L KH_2PO_4, 300 mg/L of $MgSO_4 \cdot 7H_2O$, 180 mg/L of $CaCl_2 \cdot 2H_2O$ and 1 mL/L trace element solutions I and II. Trace element solution I was composed of 5 g/L of EDTA and 5 g/L of $FeSO_4$, whereas trace element solution II was composed of 15 g/L of EDTA, 0.43 g/L of $ZnSO_4 \cdot 7H_2O$, 0.24 g/L of $CoCl_2 \cdot 6H_2O$, 0.99 g/L of $MnCl_2.4H_2O$, 0.25 g/L of $CuSO_4 \cdot 5H_2O$, 0.22 g/L of $NaMoO_4 \cdot 2H_2O$, 0.19 g/L of $NiCl_2 \cdot 6H_2O$, 0.21 g/L of $NaSeO_4 \cdot 10H_2O$ and 0.014 g/L of H_3BO_4 • 0, 50, 100, 150 and 200 mg/L GO.	• 35ºC and pH 7.5. O_2 was purged. • Reaction times of 0, 1, 2, 3 and 4 h. • Nitrite and nitrate were determined by using ion-exchange chromatography. Ammonia by a selective electrode. • Since it was observed that the bacteria reduced GO, further experiments were performed with 0, 50, 100, 150 and 200 mg/L of RGO and a cell extract, resulting of the biomass lysis. In this extract, the activity of three key enzymes (hydrazine dehydrogenase, nitrate reductase and nitrite reductase) was studied. 0, 25, 50 and 100 mg/L of exogenous coenzyme Q was added to improve the activity of the dehydrogenase, and their effects were compared with those of RGO.	• For a given GO concentration, NH_4-N, NO_2-N and total nitrogen in the mineral medium decreased with increasing the reaction time. • For a given reaction time, NH_4-N, NO_2-N and total nitrogen went through a minimum with nanomaterial concentration at 100 mg/L GO. • The colour of the solution changed from brownish yellow to black after anammox biomass addition, indicating reduction of GO. • The higher the RGO concentration, the higher the activity of hydrazine dehydrogenase, nitrate reductase and nitrite reductase. But it seems that the activity of the two first enzymes reached a plateau beyond 100 – 150 mg/L of GO. • For a given concentration between 25 and 100 mg/L, GO was more effective in improving the activity of the hydrazine dehydrogenase than the coenzyme Q.

Table 2. Published literature related to GFNs and autotrophic removal of inorganic nitrogen (continuation).

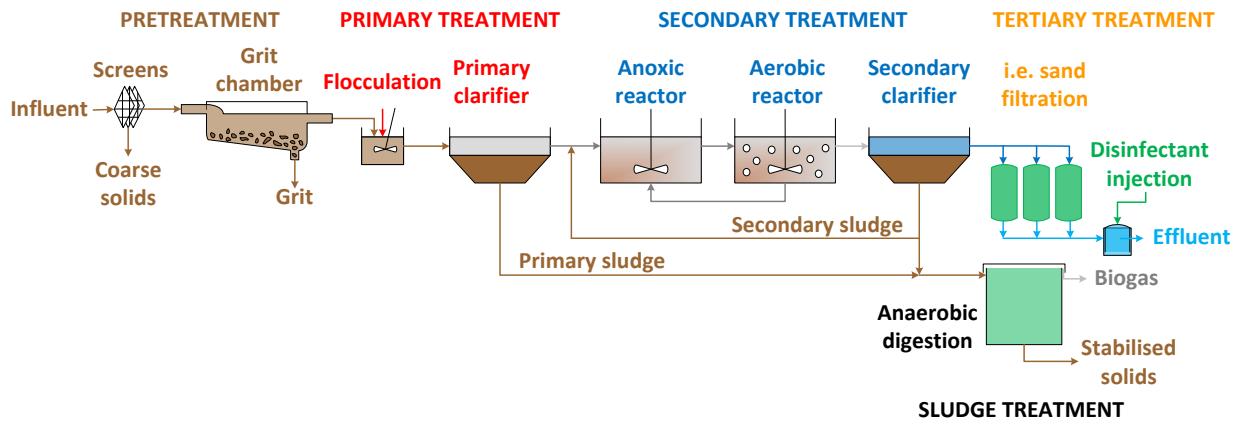| REFERENCE	MATERIALS	TESTS AND MEASUREMENTS	RESULTS
[64].	• Activated sludge from Lingshui WWTP (Dalian, China), with 4960 mg/L of VSS, inoculated in two up-flow column reactors. • The same synthetic wastewater than Yin et al. [63] but with variable amounts of NH_4-N and NO_2-N. • One sludge contained 100 mg/L of RGO.	• The oxygen of the wastewater was purged before feeding. Temperature and pH in the reactors were maintained at 35ºC and 7.0, respectively. • For the first 70 days, the wastewater contained 65 mg/L of NH_4-N and 50 mg/L of NO_2-N, and was feed at 0.05 L/h. From day 70 to 165, NH_4-N and NO_2-N were increased stepwise to 100 and 130 mg/L, respectively, maintaining the flow. From day 165 to 229, the flow was augmented stepwise to 0.081 L/h. • Nitrite and nitrate were quantified through ion-exchange chromatography, NH_4-N and VSS according to the standard methods, hydrazine dehydrogenase activity by spectrophotometry and the amount of cells by quantitative polymerase chain reaction and fluorescence in situ hybridization.	• After 20 days, the amounts of NH_4-N and NO_2-N in the effluent of the reactor with RGO were lower than those in the effluent of the reactor without RGO. The start-up lasted 49 days with RGO and 67 days without RGO. • From day 70 to 229, the nitrogen removal rate was higher in the sludge that contained RGO. • Hydrazine dehydrogenase activity and quantitative polymerase chain reaction were evaluated in days 50, 100, 150 and 200 for the two reactors. In all the cases, both the enzyme activity and the anammox bacterial growth were improved by the presence of the graphene material. • Fluorescence in situ hybridization was carried out only in days 0 and 200. In the beginning, the portion of anammox bacteria in the seed sludge was small (1.47%). After 200 days, they became the dominant population (51.3% without RGO and 62.9% with RGO).

Table 2. Published literature related to GFNs and autotrophic removal of inorganic nitrogen (continuation).

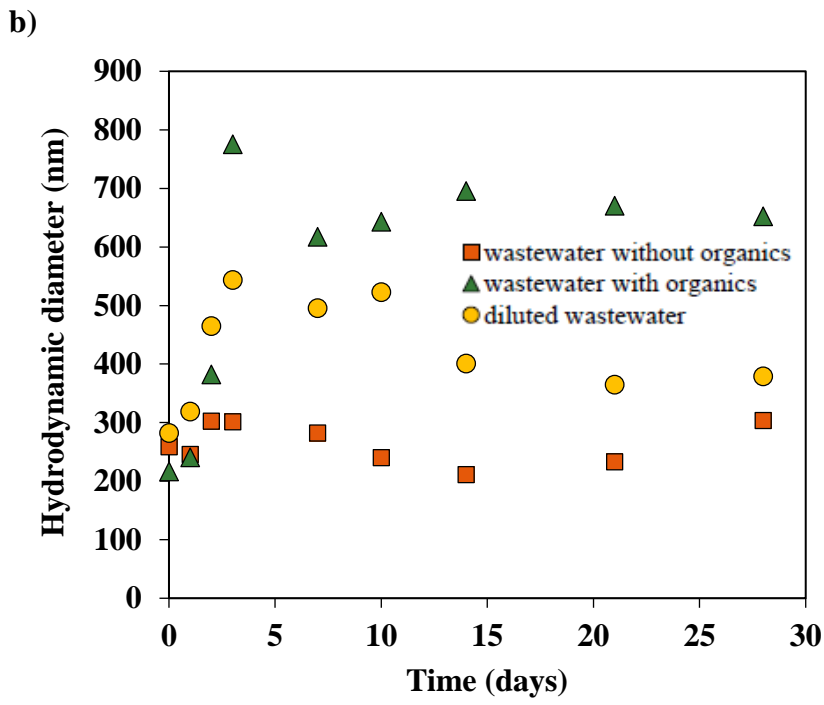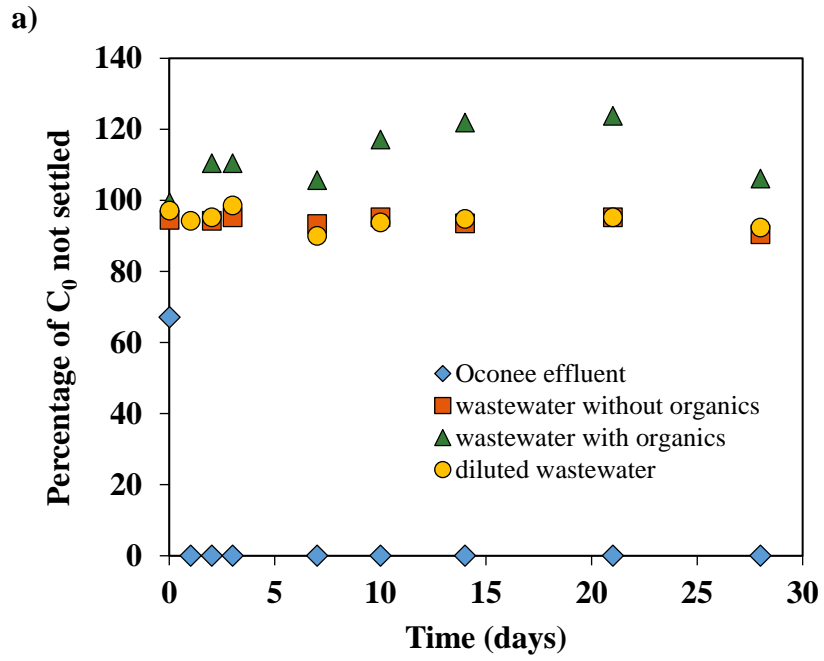| REFERENCE	MATERIALS	TESTS AND MEASUREMENTS	RESULTS
[65].	- A three dimensional bioelectrochemical denitrification system, started with anaerobic sludge (3500 mg/L of TSS) from the Erlangmiao Municipal WWTP (Wuhan, China) and operated for 200 days. - The synthetic wastewater contained 500 mg/L of NO_3-N, 500 mg/L of HCO_3^-, 10 mg/L of $MgCl_2$, 0.5 mg/L of $ZnCl_2$, 2 mg/L of $CoCl_2$, 1 mg/L of $MnSO_4$, 0.3 mg/L of $NiCl_2$, 0.3 mg/L of $CuCl_2$, 0.2 mg/L of $FeSO_4$, 0.5 mg/L of $CaCl_2$ and 0.3 mg/L of Na_2MoO_4. 0 mg/L of GO the first 50 days, 50 mg/L of GO from 50 to 100 days, 100 mg/L of GO from 100 to 150 days and 150 mg/L of GO from 150 to 200 days.	- Wastewater was pumped at 2.5 L/h. Electrical current, pH and temperature were maintained at 100 mA, 7.0 and 25ºC, respectively, for 200 days. - Nitrites and nitrates were measured spectrophotometrically, nitrogen gas and sulfates by chromatography. Lactate dehydrogenase (an indicator for cell membrane integrity) and ROS were determined by assay kits. - Genetic analyses were carried out to measure the community diversities and to taxonomically classify the bacteria. The three functionally denitrifying genes *napA* (nitrate reductase gene), *nirS* and *nirK* (nitrite reductase genes) were also evaluated.	- When GO concentration increased from 0 to 100 mg/L, the nitrate removal efficiency slightly decreased from 99.52% to 94.81%. When GO raised from 100 to 150 mg/L, the NO_3-N removal efficiency dramatically fell to 74.95%. The concentration of intermediate products, SO_4-S and NO_2-N remained almost constant, around 175 and 0 mg/L, respectively. The measured N_2 concentration showed that nitrate yielded (almost completely) gaseous nitrogen. - Both lactate dehydrogenase release and ROS production increased with GO concentration. - Microbial diversity indexes indicated that the higher the GO concentration, the lower the diversity of the microbial community. - The main phyla at 0 mg/L GO were *Proteobacteria* (36.89%), *Actinobacteria* (12.10%) and *Firmicutes* (39.06%). The first two ones decreased when increasing the GO concentration, whereas the third one increased. At 150 mg/L GO, there were 31.59% *Proteobacteria*, 1.98% *Actinobacteria* and 63.99% *Firmicutes* - On the class level, there were 51.72% *Clostridia*, 12.70% *Alphaproteobacteria*, 7.62% *Gammaproteobacteria* and 2.22% *Betaproteobacteria* at 0 mg/L GO. At 150 mg/L, there were 31.13% *Clostridia*, 7.92% *Alphaproteobacteria*, 3.21% *Gammaproteobacteria* and 31.16% *Betaproteobacteria*. - Concentration of *napA*, *nirS* and *nirK* only decreased at 100 and 150 mg/L GO, although the fall is lower for *napA* than for other two genes.

Figure 1

Figure 1

Figure 2

FIGURE 2

PRETREATMENT   PRIMARY TREATMENT   SECONDARY TREATMENT   TERTIARY TREATMENT

Screens   Grit chamber   Flocculation   Primary clarifier   Anoxic reactor   Aerobic reactor   Secondary clarifier   i.e. sand filtration

Influent

Coarse solids   Grit

Disinfectant injection

Effluent

Secondary sludge

Primary sludge

Biogas

Anaerobic digestion

Stabilised solids

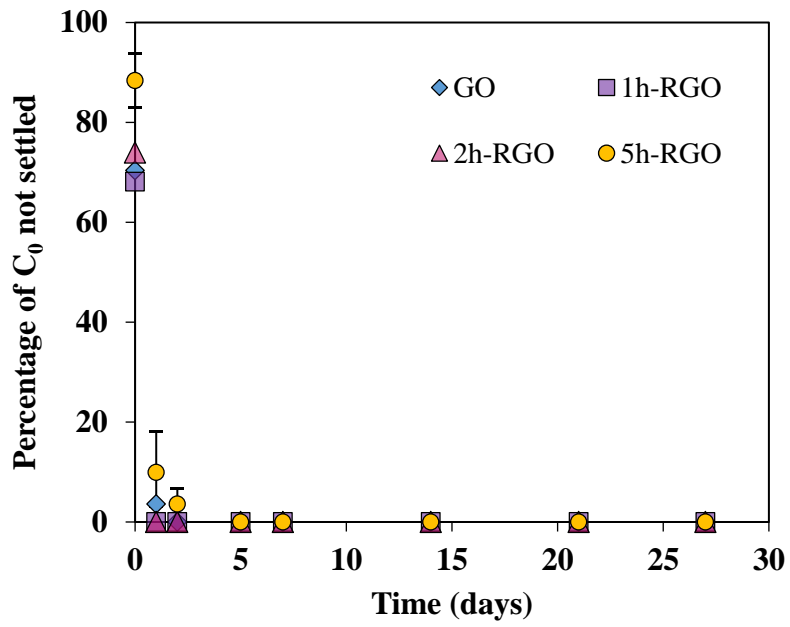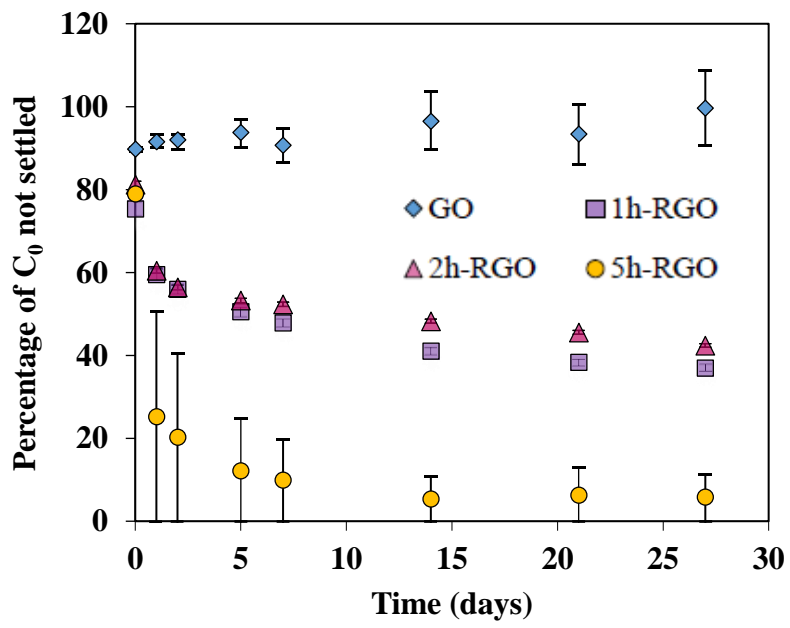SLUDGE TREATMENT

Figure 3

Figure 3

a)

b)

Figure 4

a)

b)

Figure Captions

Fig. 1. Several materials derived from the two-dimensional structure of graphene. Grey area indicates that these nanoallotropes are not included in graphene-family nanomaterials (GFNs), but constitute separated families.

Fig. 2. Flow diagram of the different stages of a WWTP.

Fig. 3. Evolution of GO concentration with time (a) and evolution of GO hydrodynamic size with time (b) in several types of wastewaters according to Chowdhury et al. [40]. Hydrodynamic diameter of Oconee effluent was not depicted since it was around 7000 nm in the first minutes and the nanomaterial was not detectable after day 1.

Fig. 4. Evolution of the concentration of GO and RGO with time in Oconee effluent (a) and synthetic wastewater without organic matter (b) according to Chowdhury et al. [41].